BRIEF REVIEW www.jasn.org

Body Fluid Dynamics: Back to the Future

Gautam Bhave* and Eric G. Neilson*†

*Division of Nephrology and Hypertension, Department of Medicine, Vanderbilt University School of Medicine, Nashville, Tennessee; and †Departments of Medicine and Cell and Molecular Biology, Feinberg School of Medicine, Northwestern University, Chicago, Illinois

ABSTRACT

Pioneering investigations conducted over a half century ago on tonicity, transcapillary fluid exchange, and the distribution of water and solute serve as a foundation for understanding the physiology of body fluid spaces. With passage of time, however, some of these concepts have lost their connectivity to more contemporary information. Here we examine the physical forces determining the compartmentalization of body fluid and its movement across capillary and cell membrane barriers, drawing particular attention to the interstitium operating as a dynamic interface for water and solute distribution rather than as a static reservoir. Newer work now supports an evolving model of body fluid dynamics that integrates exchangeable Na^+ stores and transcapillary dynamics with advances in interstitial matrix biology.

J Am Soc Nephrol 22: 2166–2181, 2011. doi: 10.1681/ASN.2011080865

Transcapillary movement of water and solute between cells and extracellular compartments interfaces with powerful physical forces residing in the interstitial matrix. A modern view of body fluid spaces hinges on reconnecting historical principles with this new and emerging dynamic.

Compartmentalization of Body Water

The content of total body water (TBW) is a physiologic function of tissue composition leading to qualitatively predictable alterations with age, gender, and body weight. Most tissues such as skin, muscle, visceral organs, and brain consist of 70 to 80% water by weight, whereas adipose tissue and bone are only 10 to 20% water. TBW reflects a weighted average of tissue water content with relatively lower values in subjects with greater adiposity or lower muscle mass. Relative to weight, women and elderly individuals generally have less body water because of higher content of body fat or preferential loss of muscle mass with age, respectively. TBW increases with obesity but decreases relative to body weight with the gain of relatively drier adipose tissue.[1,2]

Nephrologists routinely estimate TBW to gauge electrolyte and fluid deficits with hypovolemia or hypertonicity, assess dialytic adequacy using TBW as a surrogate for the volume of distribution of urea, guide drug dosing, and rationalize dialytic clearance of toxins. TBW is classically estimated as 60% of body weight in men and 50% of body weight in women deducting 5% for elderly patients.[3] Given physiologic variation in body tissue composition, early investigators recognized that absolute weight-based rules of estimation apply only to a select population of healthy individuals[4] and subsequently derived regression equations better predict TBW in a broader range of subjects. Anthropomorphic equations including age, gender, ethnicity, weight, and height are now available to im-

Published online ahead of print. Publication date available at www.jasn.org.

Correspondence: Dr. Gautam (Jay) Bhave, Division of Nephrology and Hypertension, Department of Medicine, S3223 Medical Center North, Vanderbilt University School of Medicine, Nashville, TN 37232-2372. Phone: 615-322-4794; Fax: 615-343-7156; E-mail: gautam.bhave@vanderbilt.edu

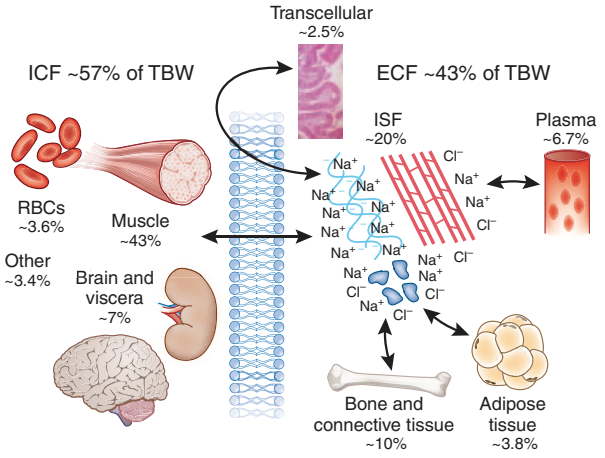

Figure 1. Body fluid compartments. In the "average" adult man, intracellular fluid (ICF) and extracellular fluid (ECF) domains consist of about 57 and 43% of total body water (TBW). The ECF compartment is further subdivided into interstitial fluid (ISF)/lymph, plasma, bone and connective tissue, adipose tissue, and transcellular water. Skeletal muscle predominates the ICF. Percentages are percent of TBW. Adapted from references [2] and [27]. RBCs, red blood cells.

prove the accuracy of estimation (see supplemental material).[5–7]

A simple approach to compartmentalization divides body water into extracellular fluid (ECF) and intracellular fluid (ICF) domains (Figure 1). ECF is subdivided into five subcompartments: plasma volume; interstitial and lymph fluid; dense connective tissue and bone; transcellular fluid within body cavities such as the pleural space, cerebrospinal fluid system, peritoneal cavity, and recirculating ductal secretions from the gastrointestinal tract; and adipose tissue.[2,8] Scant adipose tissue water resides primarily in the ECF and tips compartmentalization toward the extracellular compartment with increasing obesity. Higher fat mass and lower skeletal muscle content raises relative ECF to 45 to 48% of TBW in women, whereas the converse shifts ECF closer to 42 to 45% of TBW in men. Morbid obesity may result in the relative expansion of ECF up to 50 to 60% of TBW.[4,8–10]

No experimental technique perfectly measures ECF or its components. The distribution volume of saccharides (inulin, sucrose, and mannitol), anions (thiocyanate, thiosulfate, sulfate, bromide, and chloride), and sodium has been used to estimate ECF water. These volumes encompass different anatomic and functional spaces (Table 1).[2,11–14] When corrected for intracellular entry (approximately 10%), the distribution volume of halides best estimates ECF at approximately 42 to 48% of TBW depending on age and gender (approximately 45% as a population average).[4,11,14,15] Delineating the exact distribution of ECF among its compartments requires an integration of classic tracer distribution volumes with anatomic data including classic human dissection and chemical tissue analysis or more recent imaging techniques.[16] Consistent estimates of plasma, interstitial, transcellular, and adipose ECF volumes have been delineated despite varying data sources over time (Figure 1).[2,4,14,16,17] Dense connective tissue and bone pose technical difficulties, particularly with the accurate separation of connective tissue, muscle, and marrow from bone, variation in bone preparation (± marrow, ± articular cartilage, cortical, or trabecular bone), and significant loss of water with age.[14,18] Edelman and Leibman[2] drew upon historic dissection data for skeletal water as 16% of body weight,[19] skeletal water content as 25 to 30% by weight,[20–23] and assumed skeletal water is >90% extracellular to calculate ECF bone water as 7.5% of TBW. Unfortunately, skeletal water is not >90% extracellular, because skeletal weight includes bone and enclosed marrow (Table 2).[17,18,24,25] Normally active bone marrow is highly cellular, predominantly intracellular water.[25,26] When bone and marrow are accounted for, skeletal water is only about 60% extracellular, reducing bone ECF to 3% of TBW (Table 2).

Skeletal muscle water is often underappreciated but accounts for 40 to 50% of TBW, nearly 75% of ICF and cell mass, and about 33% of interstitial fluid volume. Loss of muscle mass redistributes TBW from ICF to ECF and increases the ratio of plasma to interstitial fluid volume.[4,27] To clarify the compartmentalization of body water, we provide a balance sheet for body weight and water distribution among the major body tissues for men and women (Table 3).

Forces Governing Water Distribution

Hydrostatic pressure and osmosis drive water between the ECF and ICF compartments, and the eventual body water distribution reflects a steady state of these forces[28]:

$$P_{ic} - P_{ec} = \Pi_{ic} - \Pi_{ec} \qquad \text{(Eq. 1)}$$

P_{ic} and P_{ec} represent intracellular and extracellular hydrostatic pressures, respectively, and Π_{ic} and Π_{ec} represent os-

Table 1. Tracer distributions for measurement of ECF volume

Tracer	Volume of Distribution (% TBW)	Plasma/Lymph/ Interstitium	Connective Tissue	Bone	ICF
Saccharides					
inulin	25 to 33	+++	0	+	0
sucrose	30 to 36	+++	+	++	0
mannitol	33 to 39	+++	++	++	0
glucose	42 to 46	+++	++	+++	+ (~10%)
Sulfate	33 to 39	+++	++	++	0
Chloride (or bromide)	46 to 52	+++	++	+++	+ (~10%)
Sodium	50 to 55	+++	++++	++++	0 (~3%)

0, <5%; +, 5 to 35%; ++, 35 to 75%; +++, 75 to 125%; ++++, >125% penetration. Adapted from references [2,11–15], and [182]. TBW, total body water; ICF, intracellular fluid; ECF, extracellular fluid.

Table 2. Distribution of water and Na^+ within bone and marrow (skeleton)

Skeletal Component	Water Content (L)	Relative Water (% of Tissue Mass)	ECF Water (L)	Relative ECF (% of TBW)	Na^+ Content (mEq/kg of body weight)	Tissue [Na^+] (mEq/L H_2O)
Bone	0.9	15	0.9	2.1	18 to 20 (5)	~1500 (~400)
Active marrow	0.9	80	0.18	0.4	0.4	30
Inactive marrow	0.4	15	0.32	0.75	0.6	110
Total	2.2	23	1.4	3.25	21 (6)	700 (200)
Tissue water (%)			63			

The values are estimates for average adult man. The values in parentheses represent exchangeable Na^+ as opposed to total Na^+. Based on references [10,14,18,25,26,183]. TBW, total body water; ECF, extracellular fluid.

Table 3. Body water distribution among tissues

Tissue	Weight (kg)	Body Weight (%)	Water Content Fraction	ECF Fraction	ECF Water (L)	ICF Water (L)	Total Water (L)
Blood							
man	5.5	7.53	0.80	0.63	2.79	1.61	4.40
woman	4.1	6.83	0.80	0.68	2.23	1.05	3.28
Skeletal muscle							
man	28.5	39.04	0.76	0.16	3.47	18.19	21.66
woman	18	30	0.76	0.16	2.19	11.49	13.68
Skin							
man	4.3	5.89	0.72	0.95	2.94	0.15	3.10
woman	3	5	0.72	0.95	2.05	0.11	2.16
Brain and viscera							
man	6	8.22	0.72	0.35	1.51	2.81	4.32
woman	5.4	9	0.72	0.35	1.36	2.53	3.89
Bone							
man	5.75	7.88	0.15	1.00	0.86	0.00	0.86
woman	4.2	7	0.15	1.00	0.63		0.63
Active Marrow							
man	1.17	1.6	0.80	0.20	0.19	0.75	0.94
woman	0.9	1.5	0.80	0.20	0.14	0.58	0.72
Inactive Marrow							
man	2.48	3.4	0.15	0.80	0.30	0.07	0.37
woman	1.8	3	0.15	0.80	0.22	0.05	0.27
Connective Tissue							
man	3.7	5.07	0.80	1.00	2.96	0.00	2.96
woman	3	5	0.80	1.00	2.4	0.00	2.4
Transcellular							
man	1.1	1.51	0.95	1.00	1.05	0.00	1.05
woman	1.1	1.83	0.95	1.00	1.05	0.00	1.05
Adipose Tissue							
man	14.5	19.86	0.14	0.80	1.62	0.41	2.03
woman	18.5	30.83	0.13	0.85	1.97	0.35	2.31
Total							
man	73				17.69	24	41.68
woman	60				14.23	16.15	30.38
% of TBW							
man					42.43	57.57	
woman					46.84	53.16	
% of Body Weight							
man							57.1
woman							50.6

The values shown are for an average adult man or an average adult woman. Adapted from references [1,2,4,10,14,16–18,25,26], and [184–186]. TBW, total body water; ICF, intracellular fluid; ECF, extracellular fluid.

motic pressures. Plants, fungi, and bacteria possess rigid cell walls that generate hydrostatic pressure to counteract osmotic pressure gradients. Animal cells shed these reinforced walls during evolution to gain flexibility, but the cost of this loss leaves cell volume regulation to the mercy of extracellular tonicity[29,30]:

$$P_{ic} - P_{ec} = 0 \quad \text{(Eq. 2)}$$

$$\Pi_{ic} = \Pi_{ec} \quad \text{(Eq. 3)}$$

$$\Pi\,(37°C; \text{mmHg}) = 19.34 * \varphi * z * [c] \quad \text{(Eq. 4)}$$

$$\text{Osmolality (mOsm/kg)} = \varphi * z * [c] \quad \text{(Eq. 5)}$$

where [c] represents molal solute concentration, z is the valence for electrolyte solutes, and φ is the osmotic coefficient for nonideality (see supplemental material for further details and index of mathematical symbols).[31,32]

Osmotic water movement is directly proportional to hydraulic permeability (L_p) and solute concentration gradient ($\Delta[c]$) in the ideal situation of an impermeable solute[33]:

$$\text{Osmotic Water Flux} = L_p * \Delta\Pi_{ideal} = L_p * 19.34 * \varphi * z * \Delta[c] \quad \text{(Eq. 6)}$$

Most solutes are partially permeable and undergo convective transport along with water. Staverman introduced the *reflection coefficient*, σ, to relate the observed osmotic pressure gradient ($\Delta\Pi_{obs}$) to the ideal osmotic pressure gradient ($\Delta\Pi_{ideal}$) with an impermeable solute[34]:

$$\sigma = \frac{\Delta\Pi_{obs}}{\Delta\Pi_{ideal}} \quad \text{(Eq. 7)}$$

$$\text{Osmotic Water Flux} = L_p * \sigma * 19.34 * \varphi * z * \Delta[c] \quad \text{(Eq. 8)}$$

σ is a dimensionless number between 0 and 1. In the presence of a concentration gradient, a solute with $\sigma = 1$ produces maximal osmosis, whereas a solute with $\sigma = 0$ fails to generate osmotic water movement. Why is there no net water flux when $\sigma = 0$ despite a large concentration gradient ($\Delta[c] \gg 0$)? Qualitatively, solute movement down its concentration gradient provides free energy for water to move against its osmotic gradient, which counteracts favorable water movement in the opposite direction; thus, no *net* water transport results. For solute to provide free energy for uphill water movement, both solute and water must move in a *coupled* fashion along the same pathway.[35]

Solutes are often classified as *effective* or *ineffective* osmoles on the basis of their ability to generate osmotic water movement. Osmotic water flux requires a solute concentration gradient ($\Delta[c] \gg 0$) and a sizeable reflection coefficient ($\sigma \gg 0$); effective osmoles satisfy both requirements, whereas ineffective osmoles fail on one or both counts. Simplistically, a solute concentration gradient across a membrane barrier must be generated faster than the solute flux across the barrier to sustain a concentration gradient for osmosis. Flux of noncharged solutes is often divided into a diffusive component in the absence of water movement and a convective component, which occurs with water flux (J_v)[33,36]:

$$J_s = \underbrace{P_D * \Delta[c]}_{\textit{Diffusive}} + \underbrace{(1 - \sigma) * J_v * [c]_m}_{\textit{Convective}} \quad \text{(Eq. 9)}$$

where J_s is solute flux, P_D is diffusive permeability, and $[c]_m$ is mean solute concentration across the membrane. Generally, solutes with low reflection coefficients ($\sigma \rightarrow 0$) have high P_D, because the transport pathway allowing for convective solute transport with water also typically supports diffusive solute movement.[37] The converse is not necessarily true because solutes with high reflection coefficients ($\sigma \rightarrow 1$) may or may not exhibit low P_D depending on the characteristics of the independent pathway for solute diffusion. If the independent pathway is simple diffusion through the lipid bilayer, P_D is typically low.[38] Alternatively, if the independent pathway is transporter facilitated, P_D is relatively high. For example, along inner medullary collecting ducts, urea and water move independently through urea transporter and aquaporin facilitated pathways during high ADH states; thus, P_D is high, but σ is near 1.[39,40]

Urea illustrates the relationship between solute osmotic efficacy and membrane permeability, diffusion surface area, and kinetics of solute generation or loss. Urea is relatively hydrophilic and exhibits low P_D (~ 1 to 5×10^{-6} cm/s) and a reflection coefficient near 1 in artificial lipid bilayers; thus, urea is quite effective at eliciting osmosis when urea concentration gradients are *abruptly* created in these experimental systems.[41] This is in contrast to ethanol, which exhibits high P_D ($\sim 10^{-4}$ cm/s) even with model membranes.[42] However, textbooks often suggest that urea is freely diffusible across membranes and therefore an ineffective osmole.[3] Urea transporters facilitate urea diffusion across some biologic membranes, but even the low permeability of pure lipid bilayers is sufficient to minimize urea concentration gradients as total cell membrane surface area is quite large ($\sim 1.2 \times 10^8$ cm^2 or 12,000 m^2), and urea generation rate is comparatively meager.[43] Even if one assumes a robust urea generation rate of about 40 g/d, pure lipid bilayer permeability, and no urea excretion or metabolism, a transcellular urea gradient of only about 0.025 mM is expected (see supplemental material). Transcapillary urea gradients are also minimal for most capillary beds as a result of high diffusive permeability and a low reflection coefficient ($\sigma < 0.1$) with urea easily traversing interendothelial pores.[44–46] However, cerebral capillaries exhibit low urea permeability with a sizeable reflection coefficient of about 0.5.[47,48] If blood urea nitrogen falls at a rate of 50 mg/dl/h during hemodialysis, a cerebral transcapillary urea gradient of about 0.25 mM can develop leading to a $\sim$2.4 mmHg (19.34 * 0.5 * 0.25 mOsm/kg) osmotic pressure favoring capillary filtration (see supplemental material). Cerebral interstitial edema or *dialysis disequilibrium* may ensue from such a rapid fall in blood urea nitrogen.[49]

At the capillary-interstitial interface, plasma proteins are excluded from interendothelial pores and act as effective osmoles, whereas small solutes such as Na^+, Cl^-, and urea are ineffective osmoles freely moving across interendothelial spaces.[44,50] Oncotic and colloid osmotic pressure (COP) are used to describe protein-generated osmotic pressure, but these

terms unfortunately suggest a distinct mechanism. Oncotic pressure or COP are simply osmotic pressures with protein colloids as effective osmoles and smaller solutes as ineffective osmoles. We will use COP only as *shorthand* to specify measurement technique rather than biologic phenomena. Oncometers consisting of membranes impervious to protein but permeable to small solutes only measure COP as opposed to osmolality measurements on the basis of freezing point or vapor pressure, which measure osmotic pressure related to all dissolved molecules including small solutes and proteins.[51] Charged proteins generate COP not only as dissolved molecules but also through electrostatic attraction of oppositely charged small counter-ions known as a *Donnan effect*.[52] Protein charge depends on isoelectric point (pI); if pH is greater than pI, the protein is negatively charged and vice versa. Plasma albumin with a pI = ~5 is quite negatively charged at physiologic pH and attracts Na^+ and other cations. Thus, albumin COP (approximately 16 to 18 mmHg) relates to its relatively high plasma concentration and low molecular weight (4 g/dl ≅ 0.58 mmol/kg = 11.2 mmHg; effective molecular weight [MW] = 69 kD) and electrostatically associated cations (17 mmHg − 11.2 mmHg = 5.8 mmHg; ~33% of albumin COP).[45]

Plasma COP is often equated with albumin COP. Although albumin is the largest single contributor to plasma COP accounting for about 66% to 75% of the normal COP (albumin COP ≅ 16 to 18 mmHg, normal plasma COP ≅ 25 mmHg), the remaining nonalbumin plasma proteins or globulins should not be ignored particularly in hypoalbuminemic states.[45] The osmotic efficiency or the osmotic pressure per g/dL of protein can be grossly examined using an average molecular weight (MW_{av}; see supplemental material):

$$\Pi \div [\%\ \text{protein (g/dL)}] \propto 193.4 \div MW_{av} \quad \text{(Eq. 10)}$$

Proteins with higher MW_{av} are less osmotically efficient for each g/dl of protein and vice versa. Plasma albumin exhibits a MW_{av} of ~69 kD, whereas plasma globulins are less efficient with a MW_{av} of ~150 kD (see supplemental material).[45,53–55] Additionally, globulin fractions exhibit different MW_{av}: α_1 = 45 kD, α_2 = 115 kD, β = 125 kD, and γ = 145 kD.[56,57]

Analbuminemia or congenital absence of albumin is a rare human disorder (approximately 40 to 50 reported cases worldwide) recapitulated in Nagase mutant rats, which surprisingly exhibit only mild edema and low normal BP.[58–60] Plasma COP is partially maintained (approximately 50 to 60% normal) by maintaining total protein concentration in the 5 to 6 g/dl range. Equally important, the relative contributions of α and β fractions, particularly α_1, increase relative to γ globulin, increasing the osmotic efficiency of globulins with a fall in MW_{av} from ~150 kD to ~113 kD (see supplemental material).[45,58,59] Analbuminemic rats preserve plasma COP even more efficiently with near normal levels using a reduction in globulin MW_{av} from approximately 150 to ~97 kD (see supplemental material).[61]

Inflammatory hypoalbuminemia behaves similarly as α_1 and α_2 fractions—the acute phase proteins—dramatically rise, but differs compared to analbuminemia because the β fraction is *unchanged*, and the γ fraction often increases with chronicity.[62] Thus, globulin osmotic efficiency improves but slightly less compared with analbuminemia with a fall in globulin MW_{av} from ~150 kD to ~120 kD (see supplemental material). The larger osmotic contribution of plasma globulins facilitates a robust defense of plasma COP in inflammatory states and explains the superior correlation of plasma total protein concentration with plasma COP compared with serum albumin in critically ill, hypoalbuminemic patients.[63,64]

Cell Volume Homeostasis and Body Na^+ and K^+ Distribution

Tonicity is shorthand for the action of effective osmolality across a barrier and in this context traditionally refers to the volume behavior of cells in a solution. Osmolality, on the other hand, measures both effective and ineffective osmoles in a kilogram of body fluid.[65–67] For instance, ethanol elevates plasma osmolality but does not affect tonicity by rapidly permeating lipid bilayers. Thus, estimates of tonicity are physiologically relevant, whereas osmolality is an imperfect surrogate for tonicity and requires appropriate discounting of ineffective osmoles.[65–67]

The relative abundance of effective osmoles in intracellular and extracellular compartments dictates body water distribution between ICF and ECF. All cells contain largely fixed or poorly permeable anions such as metabolites (ATP, phosphocreatine, and sulfate), nucleotides, and proteins.[29] K^+ acts as the primary counter-ion and serves optimal ribosomal protein synthesis requiring high intracellular K^+ concentrations.[68] The fixed intracellular anions and K^+ counter-ions create a Donnan effect-related osmotic gradient favoring persistent water entry. To counteract this osmotic gradient, Na^+-K^+-ATPases actively extrude Na^+ ions producing a *double-Donnan effect*.[69] Cl^- passively moves with Na^+ to maintain electroneutrality leading to osmotic equilibrium (Figure 2).[29,70] In essence, the cells expend ATP to convert permeable Na^+ and K^+ ions into impermeable, effective osmoles sequestered in the ECF and ICF, respectively. Similarly, Cl^- concentrates in the ECF, whereas fixed anions predominate in the ICF.[29,71] Water passively distributes into the ECF or ICF compartments in proportion to the effective Na^+ and K^+ content to reach effective osmotic equilibrium (tonicity) and establish cell volume.

Almost 98% of total body Na^+ is distributed among the ECF subcompartments (Table 4). Total body Na^+ is often divided into exchangeable (Na^+_{ex}) and nonexchangeable domains on the basis of the extent of radioisotope Na^+ equilibration with the body pool. About 20 to 30% of total body Na^+ is nonexchangeable, residing in anhydrous bone matrix.[21,72–74] Total body K^+ diametrically mirrors Na^+ with about 95% located intracellularly (Table 4). Unlike Na^+, however, over 90% of body K^+ is exchangeable.[75] To-

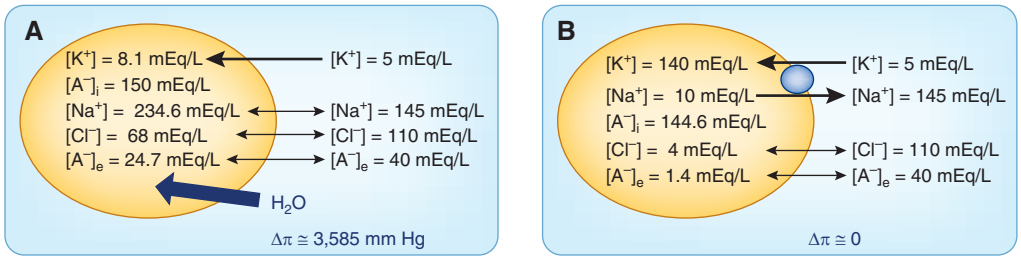

Figure 2. Double-Donnan effect and cell volume homeostasis. (A) Fixed intracellular anions (A^-) create a large Donnan effect-related osmotic pressure favoring untenable water entry. (B) The Na^+/K^+ ATPase essentially fixes Na^+ ions extracellularly to create a Na^+-related Donnan effect. The Na^+ and fixed anion effects counteract one another to form a double-Donnan steady state with no transmembrane osmotic gradient. Adapted from reference [29].

Table 4. Body sodium and potassium distribution

	Plasma		Interstitium		Bone and Connective Tissue		Intracellular		Total (mEq/kg)	Exchangeable (mEq/kg)
	Content (mEq/kg)	Concentration (mEq/kg H_2O)	Content (mEq/kg)	Concentration (mEq/kg H_2O)	Content (mEq/kg)	Concentration (mEq/kg H_2O)	Content (mEq/kg)	Concentration (mEq/kg H_2O)		
Na^+	6	150	18	148.5	28 (14)	400 (200)	2	6	54	40
K^+	0.2	4.2	0.5	4	3.3	4.8	52.6 (49.3)	160 (150)	56.6	53.3

The values are estimates for an average adult man. The parentheses indicate exchangeable cation opposed to total cation content and concentration. Adapted from references [2,14,183], and [187].

tal body K^+ is proportional to cell mass and reflects metabolic activity. Red blood cell volume supplies oxygen for tissue metabolism and expectedly correlates with total body K^+.[76] Chronic diseases with wasting or inflammation demonstrate proportionate declines in body cell mass, total body K^+, and red blood cell volume.[4]

Extracellular Fluid Dynamics

New studies suggest that the plasma and lymphatic compartments and the interstitium are dynamic interfaces for water distribution. ECF is heterogeneous, yet plasma, representing approximately 17% of ECF, is used to assess body fluid homeostasis. Neurohormonal and renal homeostatic mechanisms sense and defend effective circulating blood volume, a poorly measurable quality of arterial filling determined primarily by blood volume, cardiac output, and vascular tone.[77] The kidney primarily modifies sodium balance in response to effective circulating blood volume derangements.[78–80] Although the kidney's set point focuses on the vascular compartment, its homeostatic response affects the entire ECF as sodium distributes throughout this compartment. Thus, only the vascular compartment is actively regulated, whereas homeostasis of the significantly larger extravascular ECF, particularly the interstitium, depends primarily on local autoregulation.[80,81]

Unlike the tonicity equilibrium between cells and their surrounding environment, plasma volume is maintained as a nonequilibrium steady state with net water loss into interstitium and an equivalent water gain caused by lymphatic drainage from interstitium back into plasma. About 8 L/d of capillary filtrate moves into lymphatics with about 4 L reabsorbed in lymph nodes and the remainder returning to the circulation through the thoracic duct.[82] Although capillary filtration has historically dominated investigation, interstitial balance equally depends on lymphatic function.[81] The modified Starling relationship mathematically delineates water flux between capillary plasma and interstitium[36,45,83]:

$$\text{Net Capillary Filtration } (J_v) = L_p * [(P_c - P_i) - \sigma (\Pi_c - \Pi_i)] \quad \text{(Eq. 11)}$$

where L_p is hydraulic permeability, P_c and P_i are capillary and interstitial hydrostatic pressures, Π_c and Π_i are capillary and interstitial colloid osmotic pressures, and σ represents the osmotic reflection coefficient. At steady state, capillary filtration must equal lymphatic flow. The magnitude of hydrostatic and osmotic pressures and their balance across capillaries has been debated continuously over the last century. Physiology textbooks still present a framework where filtration predominates at the arterial end and reabsorption occurs at the venous end of the capillary with falling capillary hydrostatic pressure and constant capillary osmotic pressure (Figure 3).[3,45] Recent studies, however, point to low net filtration with net filtration pressures (J_v/L_p) of 0.5 to 1 mmHg across the entire length of the capillary in most vascular beds (Figure 3).[84] A better understanding of interstitial matrix and reassessment of Π_i and P_i has driven this paradigm shift.

Interstitial and connective tissues are typically modeled as *triphasic* systems[85]: free flowing fluid with albumin, a gel phase with glycosaminoglycans (GAGs), and a collagen-based matrix (Figure 4). Water and small solutes (Na^+, Cl^-, and urea) move easily between all compartments according to prevailing osmotic, hydrostatic, and electrochemical forces.[86] Albumin is excluded from the GAG compartment, and both GAGs and albumin are excluded from the collagen matrix.[87,88] GAGs generate osmotic pressure (Π_{GAG}) both in proportion to concentration and negative charge density as the latter attracts cations

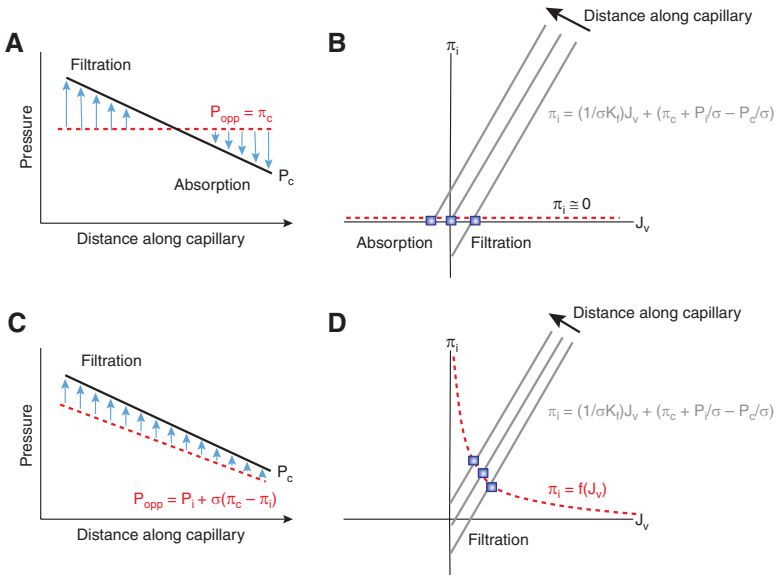

Figure 3. Paradigm shift in transcapillary fluid exchange. (A and B) Classic view of transcapillary Starling forces with Π_i and P_i ignored leading to predominant filtration on the arterial end giving way to absorption on the venous end. (C and D) Π_i is a nonlinear function of filtration rate (J_v). Filtration rate is the intersection of this function and Π_i as a function of Starling forces. The Starling relationship is linear with a slope equal to $1/\sigma K_f$ and *y* intercept of $\Pi_c + P_i/\sigma - P_c/\sigma$. As P_c falls along the capillary, the linear Starling curve left shifts as the *y* intercept increases. The left shift is blunted by a decrease in P_i. Π_i increases with falling filtration, and the relative steepness of the nonlinear Π_i (J_v) function maintains filtration along the capillary.

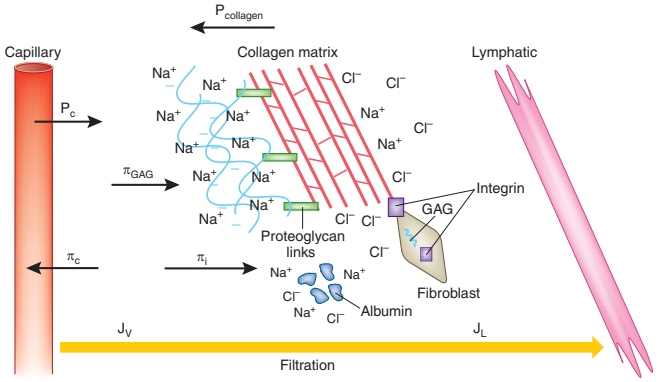

Figure 4. Triphasic interstitial model. Schematic representation of interstitial elements and their relationship to capillary forces and lymphatics. Interstitial P_i is a balance between GAG osmotic pressure (Π_{GAG}) and collagen hydrostatic pressure ($P_{collagen}$). Net capillary filtration (J_V) must equal lymphatic flow (J_L) at steady state.

and increases tissue Na^+ concentration.[85,89] The collagen matrix generates a hydrostatic pressure that typically opposes GAG osmotic swelling ($P_{collagen}$).[90,91] Except for hyaluronan, most GAGs are proteoglycans consisting of a carbohydrate GAG attached to a core protein that interacts with the collagen matrix.[92] *Measured* P_i reflects a balance between matrix hydrostatic and osmotic pressures (Figure 4)[93,94]:

$$P_i \propto P_{collagen} - \Pi_{GAG} \qquad \text{(Eq. 12)}$$

Π_i is primarily related to interstitial albumin concentration. The relative rates of water and albumin flux determine steady-state interstitial albumin concentration. Classically, albumin flux was assumed trivial compared with water flux with $\sigma \cong 1$ and interstitial albumin concentration and $\Pi_i \cong 0$. However, approximately 50 to 60% of albumin content resides in the extravascular compartment at a concentration of about 1 to 1.5 g/dl with 10 g of albumin moving from plasma to lymph per hour.[82] Because GAGs and collagen exclude albumin from about 25 to 50% of the interstitial volume,[88,95] the *effective* albumin concentration in the interstitium approaches 2 to 3 g/dl. Π_i is 30 to 60% of Π_p when directly measured and mirrors *effective* albumin concentration. Filtration rate dynamically regulates Π_i with increased filtration diluting interstitial albumin and lowering Π_i and absorption raising Π_i.[96] Π_i changes steeply with filtration rate as water flux outstrips albumin flux, and albumin exclusion falls producing a disproportionate decline in effective albumin concentration compared with dilution alone.[88]

Interstitial protein gradients produce an even steeper nonlinear fall in Π_i with filtration rate. In a two-pore model, most filtration occurs through small pores with $\sigma_{albumin} \cong 0.95$, whereas large pores transport a minute fraction of water but allow for significant albumin convection with large pore $\sigma_{albumin} \cong 0.05$.[97] Effective albumin concentration in close proximity to small pores determines filtration as albumin infusion into the general pericapillary interstitium minimally affects filtration.[98,99] Albumin gradients develop with high concentrations around large pores and low concentrations near small pores (Figure 5).[100] Whether diffusion between pore regions is limited enough to sustain substantial protein concentration gradients is unclear. A variation of the theme proposes endothelial glycocalyx as the primary interendothelial, small pore permeability barrier with subglycocalyx Π as the primary determinant of filtration; restricted access to the subglycocalyx space may further limit albumin diffusion to amplify interstitial concentration gradients.[101]

Interstitial hydrostatic pressure (P_i) is slightly negative to zero (−4 to 0 mmHg).[93,96,102,103] At euvolemia, the interstitium behaves as a low compliance system; small increases in interstitial volume or capillary filtration rate are met with a steep increase in P_i which counteracts capillary filtration and edema. However, once interstitial volume rises by approximately 20 to 50% or P_i is slightly positive, the interstitium becomes highly compliant. Large changes in volume now min-

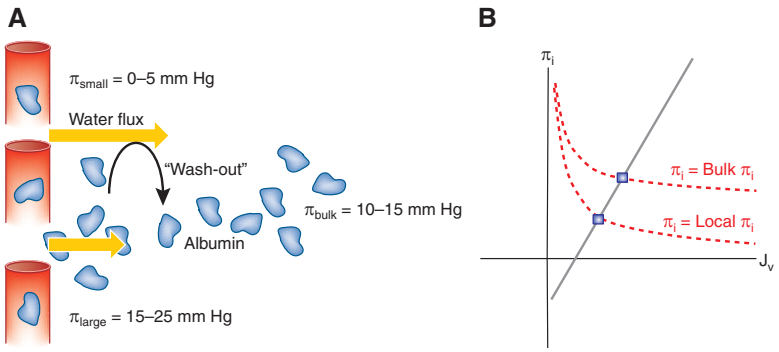

Figure 5. Effect of local interstitial protein gradients on Π_i. (A) Schematic of two pore model where albumin primarily moves through large pores leading to high albumin concentration near large pores and low concentration near small pores. Local interstitial osmotic pressure will primarily reflect osmotic pressure in the vicinity of the small pore, which is lower than bulk osmotic pressure. Increasing filtration rate will more steeply decrease local osmotic pressure as albumin wash-out increases around the small pore. (B) Qualitative interstitial osmotic pressure (Π_i) *versus* filtration rate (J_v) curves. When Π_i equals bulk Π_i, no interstitial protein concentration gradients exist leading to higher Π_i, and shallower dependence on J_v as albumin "washout" is less effective. When Π_i reflects local Π_i with a significant protein gradient between small and large pores, the effective Π_i is lower and more steeply dependent on J_v, because albumin washout occurs more efficiently in the vicinity of small pores.

imally increase P_i leading to unabated capillary filtration and edema (Figure 6).[104,105] Interstitial cells dynamically regulate P_i shifting the entire P_i-interstitial volume curve. Cells loosen or tighten their grip on collagen matrix through cell surface integrin receptors, which interact with the extracellular matrix and the force-generating actin cytoskeleton.[106,107] Reducing collagen β1-integrin receptor interactions and/or cytoskeletal depolymerization dramatically shifts the P_i-volume curve rightward (Figure 6). Inflammatory states and thermal injury decrease P_i as a result of reduced integrin binding of collagen and/or thermal denaturation of collagen.[108–110] A fall in P_i may play a critical role in the early phase of sepsis- and burn-induced edema.[111,112] P_i eventually rises with interstitial fluid accumulation, whereas increased P_c and L_p and diminished σ maintain edema in the long term (Figure 6).[107]

Dynamic interstitial forces play a critical part in regulating plasma-interstitial fluid balance in pathologic states. In hypovolemia, P_c falls in vasoconstricted vascular beds leading to transient interstitial fluid absorption in a process known as *transcapillary refill*. Subsequent loss of interstitial volume concentrates albumin, increases Π_i, decreases P_i, and thus limits transcapillary refill at approximately 75 to 80% of lost plasma volume (Figure 7).[105,113,114]

Nephrotic syndrome demonstrates the interplay between serum albumin, Π_c, capillary filtration, and Π_i. Unlike other hypoalbuminemic states, in nephrotic syndrome the globulin MW_{av} rises significantly to ~215 kD because of a preferential

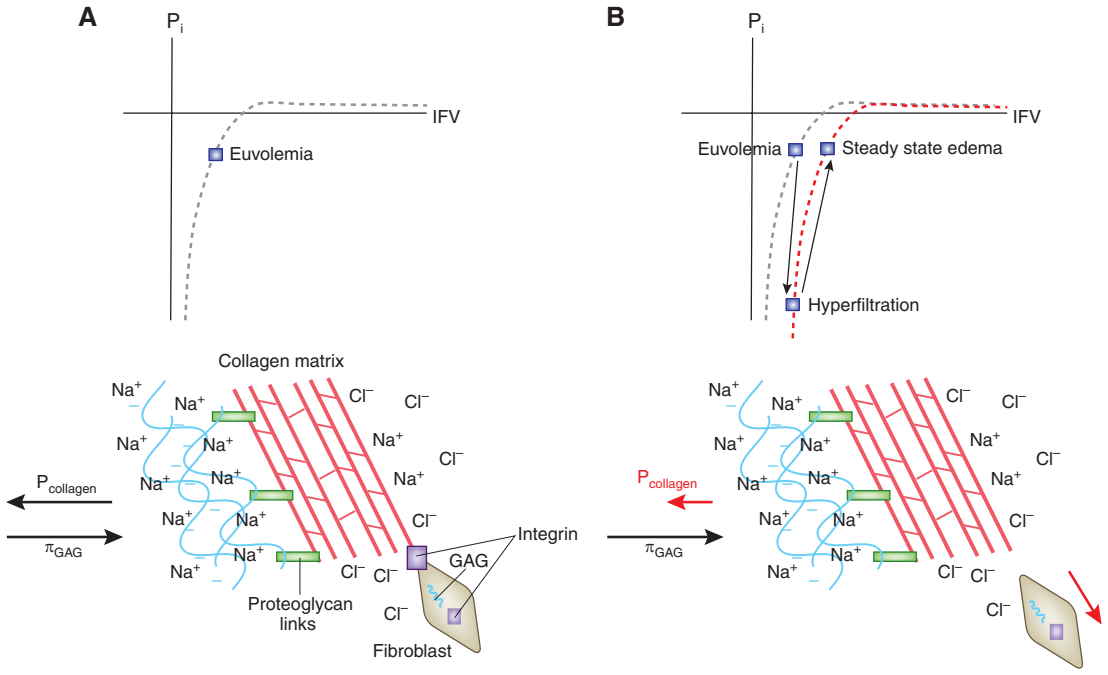

Figure 6. Dynamics of measured interstitial hydrostatic pressure P_i. (A) P_i normally varies with interstitial volume (IFV). At low IFV, compliance is low, and pressure rises significantly. Once IFV increases 20 to 50% above euvolemia, compliance increases dramatically, and P_i essentially remains near constant allowing for edema formation. (B) P_i reflects a balance between $P_{collagen}$ and Π_{GAG}. Release of integrin-mediated tension on collagen matrix decreases $P_{collagen}$ and right shifts the P_i-IFV curve, leading to increased filtration until P_i rises with edema.

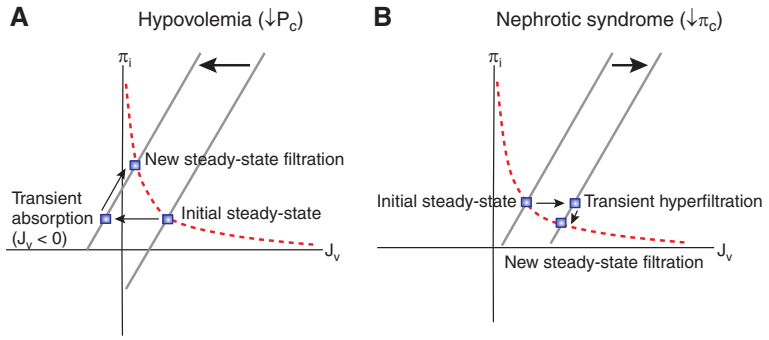

Figure 7. Transcapillary dynamics in hypovolemia and nephrotic syndrome. (A) Vasoconstriction with hypovolemia decreases P_c and left shifts the Starling Π_i curve with an increased *y* intercept. Transient interstitial fluid absorption occurs increasing Π_i and restoring a lower level of steady-state filtration. P_i also decreases leading to a small right shift in linear Starling relationship (not shown). Transcapillary refill of plasma volume occurs with absorption but may continue to occur if lymphatic flow is slow to match the lower steady-state filtration rate. (B) Π_c falls in nephrotic syndrome leading to a right shift of the Π_i Starling curve and transiently increased filtration. The subsequent fall in Π_i reduces filtration to a new steady state. P_i would increase slightly producing a left shift of the Starling linear curve to further minimize a rise in filtration (not shown).

urinary loss of osmotically efficient low molecular weight proteins along with albumin and an accumulation of high molecular proteins such as α_2-macroglobulin, fibrinogen, haptoglobin multimers, and β lipoproteins (see supplemental material).[61,62,115,116] Thus, nephrotic patients are unable to defend Π_c despite a reasonable serum total protein concentration as the globulin fraction consists of large, osmotically inefficient proteins. Π_c declines proportionately with falling plasma albumin as opposed to analbuminemic patients who exhibit approximately 50% of normal Π_c without plasma albumin. Capillary filtration rises with falling Π_c, but the subsequent fall in Π_i and rise in P_i tends to normalize filtration and minimize edema (Figure 7). The difference between Π_c and Π_i remains constant at about 50% of Π_i or about 12 mmHg, essentially negating the tendency for low Π_c to produce edema.[117,118] Of course, because the floor for Π_i is zero, once Π_c falls below 10 to 14 mmHg (around 1.5 to 2 g/dl plasma albumin), edema is inevitable.[117,119] A rapid fall in Π_c as seen in pediatric *nephrotic crises* with minimal change disease may kinetically outstrip the compensatory fall in Π_i, leading to intravascular volume depletion and hemodynamic compromise.[120–122]

Whether a fall in Π_c is the primary determinant of nephrotic edema is controversial, because several investigators have demonstrated autonomously enhanced sodium reabsorption in the distal nephron and diminished sodium excretion preceding hypoproteinemia.[123–126] Proponents of the *overfill* hypothesis suggest that renal sodium retention is the primary abnormality in nephrotic syndrome, whereas others support the *underfill* theory wherein low Π_c leads to intravascular volume depletion and secondary renal sodium retention.[127,128] Increased capillary permeability measured as albumin extravasation (increased L_p and/or decreased σ) may also contribute to intravascular volume depletion.[129] As in all controversies, individual patients may demonstrate overfill, underfill, or mixed physiology. Severe or rapidly developing hypoproteinemia and clinical features of volume depletion support underfilling, whereas hypertension, renal dysfunction, and mild to moderate hypoalbuminemia (serum albumin >2 g/dl) suggest overfilling.[128,130] Minimal change disease more commonly presents with underfill physiology, but whether histologic diagnosis is an independent predictor of volume homeostasis or simply reflects more severe or rapid hypoproteinemia with maintained GFR is unclear.[131]

Total Body and Compartmental Tonicity

Animal cells are largely in osmotic equilibrium with their surrounding environment; thus, intracellular tonicity equals interstitial tonicity.[30,132,133] Clinicians estimate plasma tonicity, which may not equal interstitial and intracellular tonicity except in the case of red blood cells ($\Pi_{RBC} = \Pi_{plasma}$). Fortunately, in most body tissues, the difference between plasma and interstitial osmolality is minimal. A direct experimental measurement of the plasma to interstitial osmolality gradient is the difference in COP, which accounts for both protein and Donnan small ion effects[96]:

$$\Pi_c - \Pi_i \cong 10\text{–}20 \text{ mmHg} \cong 0.5\text{–}1 \text{ mOsm/kg} \quad \text{(Eq. 13)}$$

The tonicity gradient between plasma and interstitium is quite small, and we can hypothesize that tonicity is equal across all body compartments:

$$\text{Plasma Tonicity} \cong \text{Interstitial Tonicity} = \text{Intracellular Tonicity} \cong \text{Total Body Tonicity} \quad \text{(Eq. 14)}$$

In addition, if we assume the vast majority of effective body osmoles are exchangeable Na^+ and K^+ and their counter-ions and glucose, the following idealized relationship is derived (see supplemental material):

$$P_{Na} = f_{PW} * \frac{Na^+_{ex} + K^+_{ex}}{TBW} - (G_{Na} * \Delta[\text{Glucose}]_p) - P_K \quad \text{(Eq. 15)}$$

where f_{PW} is the plasma water fraction, and G_{Na} is a correction factor for hyperglycemia related translocational hyponatremia that has been proposed to range from 1.5 to 2.4 mEq/L per 100 mg/dl rise in plasma glucose.[134–136]

Studies examining the relationship between exchangeable Na^+ and K^+, TBW, and P_{Na} and P_K in normal and pathologic

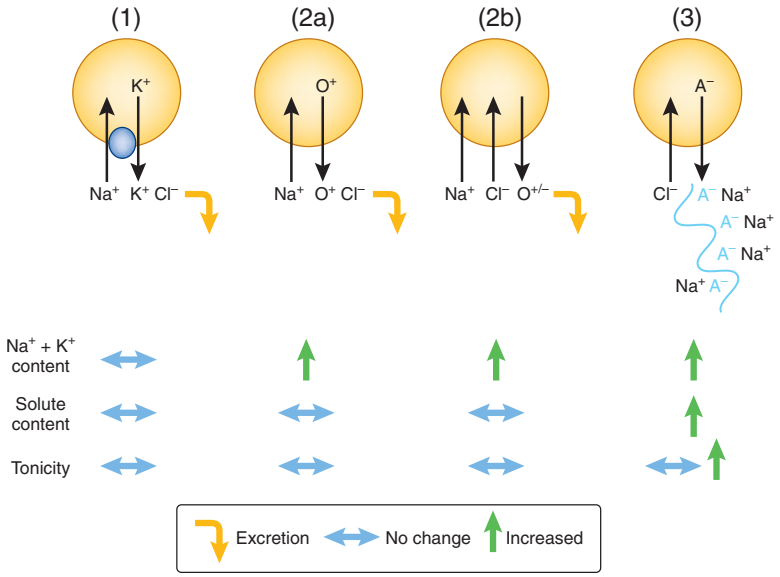

Figure 8. Mechanisms of excess sodium storage. (1) Na^+ may be exchanged for K^+, and the latter is excreted. Because total cation content is unchanged, both cation content and tonicity remain constant. (2) Positive Na^+ balance is matched by negative osmolyte (O) balance. (2a) O may be cationic (O^+; *e.g.* choline) and undergo exchange with Na^+. (2b) O may be a zwitterion (*e.g.* taurine and amino acids) or uncharged (*e.g.* sorbitol and inositol) and essentially exchange for NaCl. In both cases, cation content rises, but total solute content is unchanged. (3) Intracellular anions (A^-; *e.g.* sulfate) may be exchanged with chloride and incorporated into GAGs. Na^+ associates with GAG sulfate moieties via electrostatic interactions. Both total cation and solute content rise in this situation. Tonicity may or may not rise depending on the extent of osmole efficacy. For instance, Na^+ salts with bone mineral matrix and possibly intracellular anions may be osmotically inactive; in this case, total body tonicity is unchanged.

states have found that P_{Na} may be delineated as follows (see supplemental material):

$$P_{Na} = 1.03 * f_{PW} \frac{Na^+_{ex} + K^+_{ex} - 250}{TBW} - (G_{Na} * \Delta[Glucose]_p) - P_K \quad \text{(Eq. 16)}$$

Because total exchangeable cation ($Na^+_{ex} + K^+_{ex}$) is on the order of 90 mEq/kg, the ideal relationship is a good approximation because 250 mEq pales in comparison and 1.03 is also quite close to 1. The 250 mEq deviation from ideality relates to a small osmotic gradient between plasma and total body osmolality, non-Na^+ and K^+ osmoles besides glucose, and exchangeable *excess* Na^+ and K^+ (see supplemental material). The nonideal quantity of 250 mEq in the derived P_{Na} relationship applies only to well represented pathologic states within patient cohort data (congestive heart failure, cirrhosis, and low Na^+ diet). Whether this quantity is similar in other disease states such as syndrome of inappropriate anti-diuretic hormone (SIADH), volume depletion, and high Na^+ diet is unknown and potentially limits the accuracy of the idealized P_{Na} approximation in these situations.[137]

Broadly speaking, excess Na^+ and K^+ refer to any compartment where exchangeable Na^+ and K^+ concentration exceeds plasma water [$Na^+ + K^+$]. Often, excess Na^+ and K^+ is used interchangeably with *osmotically inactive*, although the two are not mechanistically synonomous. Some inaccurately suggest that a compartment with osmotically active Na^+ and K^+ in excess of plasma should accrue water until equilibrium with plasma is reached and excess cation is eliminated; thus, the persistence of a concentration gradient can only occur if excess cation is osmotically inactive. But excess cation may be osmotically active while maintaining a concentration gradient in two ways: a counteracting hydrostatic pressure balances the osmotic gradient, allowing compartment osmolality to differ from plasma osmolality or excess Na^+ and K^+ is counterbalanced by loss of non-Na^+ and K^+ osmolytes maintaining plasma and total body tonicity. Of course, a portion of excess Na^+ and K^+ may truly be osmotically inactive ($\varphi = 0$). Bone and a small fraction of intracellular cation probably represent the osmotically inactive pool. Some may argue that the distinction between excess and osmotically inactive cation is pure semantics, but a growing literature on cartilage suggests otherwise. Cartilage is hypertonic, yet inexorable cartilage swelling is prevented by a counteracting collagen-based hydrostatic pressure.[91,138]

Significant attention has historically focused on the dynamics of Na^+ balance given its prominent role in hypertension and edematous states. When positive Na^+ balance occurs, Na^+ is handled in several ways: Na^+ accumulates in the extracellular space with water such that plasma tonicity and Na^+ concentration remain constant; Na^+ is retained in excess of water with a resulting increase in plasma Na^+ concentration and tonicity along with a parallel rise in total body tonicity; or Na^+ is retained in excess of water with little or no change in plasma tonicity often termed *excess Na^+ storage* (or inaccurately as osmotically inactive Na^+ storage). Broadly speaking, several mechanisms account for excess Na^+ storage: negative K^+ balance offsets positive Na^+ balance such that total cation balance is unchanged; positive total cation balance ($Na^+ + K^+$) with negative balance for effective osmoles other than Na^+ or K^+ salts such that total body effective osmoles remain constant; positive cation balance with osmotically active Na^+ associating with interstitial glycosaminoglycans, thereby increasing total body tonicity relative to plasma; or positive cation balance with osmotically inactive Na^+ associating with bone mineral matrix or possibly intracellular proteins (Figure 8).

Although measuring K^+ balance is straightforward, defin-

ing other mechanisms for excess Na^+ storage is difficult. Over the last half century, investigators have debated whether the movement of Na^+ ions into or out of a storage compartment is necessary to account for positive sodium balance with high sodium diet and edematous states and negative sodium balance in volume depletion or hypotonicity. Many studies neglect K^+ balance, which can often offset a positive Na^+ balance.[139–143] Even after accounting for K^+ balance, most short term metabolic balance studies (3 to 5 days) and long term (1 to 3 months) radioisotopic studies generally find reasonable correlation between cation and water balance and plasma tonicity,[144–149] whereas intermediate balance studies (7 to 14 days) often suggest Na^+ storage.[150–152] Whether these differences reflect biologic phenomena or technical differences remains unclear.[150,153–155]

Excess Na^+ storage occurs with high sodium diet (>300 mEq/d). Some excess Na^+ exchanges with intracellular K^+ primarily from skeletal and vascular smooth muscle; thus, total cation balance in this case is unchanged.[147,156] Excess Na^+ storage in skin exceeds negative K^+ balance and has recently garnered attention, although the hypothesis dates back over 30 years in the Russian literature.[150,157,158] Animal studies demonstrate increased Na^+ concentration in skin (20 to 40 mEq/L tissue water), which translates to about 1 to 2 mEq/kg excess Na^+ storage, assuming that skin water is at most 5% of body weight.[27,156,159] Excess Na^+ may accumulate intracellularly in exchange for non-K^+ osmolytes or alternatively associate with interstitial glycosaminoglycans (Figure 8). Radiotracer Na^+ dynamics in isolated skin from animals on high sodium diets suggest an increase in the rapidly exchanging extracellular Na^+ pool rather than the more slowly exchanging intracellular Na^+ pool. Within the rapidly exchanging pool, a compartment outside the inulin space accounts for the majority of the increased Na^+ content, suggesting a sterically inaccessible site such as interstitial glycosaminoglycans.[157] Indeed, negatively charged, sulfated glycosaminoglycan content rises in skin with dietary Na^+ loading.[159–161] Na^+ loading transiently increases interstitial flow and possibly Na^+ concentration, which are known stimulators of interstitial cell matrix production, particularly sulfated GAGs.[162–165]

Na^+ associated with negatively charged purified glycosaminoglycans in cartilage exhibits an osmotic coefficient similar to normal saline; thus, skin GAG-associated Na^+ is most likely osmotically active.[86,166] Assuming that 20 to 40 mEq/L Na^+ is stored in association with skin interstitial GAGs, Π_{GAG} would rise about 100 to 200 mmHg or approximately 5 to 10 mOsm/kg to achieve the required negative charge density (see supplemental material). Typical transcapillary Starling forces pale in comparison with 100 to 200 mmHg. Dermal swelling pressures can reach up to 100 to 150 mmHg in situations where $P_{collagen}$ is reduced, suggesting that Π_{GAG} is normally quite high but counteracted by $P_{collagen}$.[111,167] Thus, Π_{GAG} can rise significantly but requires similar increases in $P_{collagen}$ to prevent high filtration rates and interstitial edema caused by low P_i ($P_i \propto P_{collagen} - \Pi_{GAG}$). Hydrostatic pressure ($P_{collagen}$) counterbalances osmotic pressure (Π_{GAG}) to eliminate water movement and maintain a small tonicity gradient between dermal interstitium and plasma. Dermal fibroblasts like their chondrocyte counterparts probably accommodate interstitial hypertonicity with osmolyte accumulation to maintain cell volume.[168,169]

When the mechanism of excess Na^+ storage across tissues is broadly surveyed, a hypothetical framework comes into view. Relatively cellular tissues such as muscle exchange Na^+ for K^+ or other intracellular osmolytes as their high cell mass relative to interstitial space provide a large osmole depot for transcellular exchange. Conversely, relatively acellular connective tissues have minimal intracellular osmoles at their disposal and alternatively depend on osmotically active storage with interstitial glycosaminoglycans or osmotically inactive storage with mineral matrix.

The Na^+ counter-anion may also modify Na^+ storage. When subjects consume large amounts of Na^+ either as Cl^- or bicarbonate (or equivalents such as citrate or ascorbate) salts, hypertension and plasma volume expansion ensues only with NaCl intake despite equivalent positive sodium balance and weight gain with sodium bicarbonate. Furthermore, NaCl consumption results in hypercalciuria, whereas sodium bicarbonate does not change urinary calcium excretion.[170–173] Taken together, water distribution tends to be extravascular and does not affect calcium homeostasis when the Na^+ counter-anion is bicarbonate. Na^+ with a base equivalent may possess a larger pool of intracellular and bone storage mechanisms. Intracellular proteins can simply titrate bicarbonate with protons with the resulting protein anionic side chain acting as a counter-ion for excess Na^+ in a potentially osmotically inactive form. For NaCl to store Na^+ in association with intracellular proteins, Na^+ would have to displace protein side chain H^+ or exchange with predominantly protein bound Ca^{2+}. The former is unlikely because cells function poorly with intracellular acidosis, whereas the latter necessitates Ca^{2+} excretion. The low solubility of calcium bicarbonate probably precludes intracellular Na^+/Ca^{2+} exchange with sodium bicarbonate but promotes bone surface crystal integration of sodium bicarbonate *in toto*. Conversely, NaCl requires Na^+/Ca^{2+} exchange at the bone matrix interface again leading to hypercalciuria.[174–176] Thus, negative Ca^{2+} balance potentially limits Na^+ storage in the setting of high NaCl intake, but not with bicarbonate salts. Although purely speculative, these hypotheses provide fertile ground for future investigation.

Alterations in intracellular, skin, and bone Na^+ storage may critically regulate blood volume homeostasis and participate in the pathogenesis of salt-sensitive hypertension. These storage mechanisms may buffer the blood volume against transient or sustained sodium loads. Animals and patients with reduced Na^+ storage capacity are prone to blood volume expansion and hypertension.[158,177,178] Alternatively, these storage mechanisms activate deleterious neurohormonal and/or inflammatory signaling pathways.[159] Although this work points to an exciting paradigm shift in blood volume regulation, whether

these mechanisms contribute to pathology broadly or in a narrow subset of patients remains unknown. Because United States dietary Na^+ intake is 150 to 200 mEq/d ± 100 mEq/d (2 SD)[179–181] and storage mechanisms regulating Na^+ homeostasis require dietary intakes exceeding 300 mEq/d,[140,150] only about 5% of essential hypertension in American patients may involve alterations in Na^+ storage.

Conclusions

Understanding body fluid dynamics is critical to the practice of medicine. Phenomenal work accomplished during the last century has lulled us into relying on aging textbook dogma or believing there is little left to discover. However, re-examination of foundational literature suggests some teachings stray from original data. The division of TBW into ICF and ECF is frequently taught as an arbitrary distribution rather than a product of cell volume homeostasis and the relative partitioning of body fat, protein, Na^+, and K^+. New investigations also suggest novel paradigms involving the dynamic nature of the interstitium that critically regulate ECF homeostasis. Although diet and the kidneys arbitrate blood volume homeostasis in the long run, the interstitium plays a larger role in short term blood and interstitial volume adjustments. Short term Na^+ storage and interstitial volume homeostasis may be relevant to transient or nonequilibrium phenomena such as BP dipping, flash pulmonary edema, rapid blood loss, burns, and sepsis, to name a few. Future investigation will hopefully unify the molecular and structural biology of interstitial cell-matrix interactions with classic Starling physiology to identify new therapeutic targets for hemodynamic derangements.

ACKNOWLEDGMENTS

The authors thank Raymond Harris, Sanjeev Shah, Peter Aronson, and Roland Blantz for comments on earlier versions of this manuscript and Sergei Chetyrkin for translation of the references in Russian.

DISCLOSURES

None.

REFERENCES

1. Fanestil DD: Compartmentation of body water. In: *Clinical Disorders of Fluid and Electrolyte Metabolism*. Fifth Ed., edited by Narins, RG, New York, McGraw-Hill, 1994, pp. 3–20
2. Edelman IS, Leibman J: Anatomy of body water and electrolytes. *Am J Med* 27: 256–277, 1959
3. Rose BD, Post TW: *Clinical Physiology of Acid-Base and Electrolyte Disorders*, New York, McGraw-Hill, 2001
4. Moore FD, Olesen KH, McMurrey JD, Parker HV, Ball MR, Boyden CM: *The Body Cell Mass and Its Supporting Environment*, Philadelphia, W.B. Saunders, 1963
5. Chumlea WC, Guo SS, Zeller CM, Reo NV, Baumgartner RN, Garry PJ, Wang J, Pierson RN Jr, Heymsfield SB, Siervogel RM: Total body water reference values and prediction equations for adults. *Kidney Int* 59: 2250–2258, 2001
6. Ellis KJ: Reference man and woman more fully characterized: Variations on the basis of body size, age, sex, and race. *Biol Trace Elem Res* 26–27: 385–400, 1990
7. Watson PE, Watson ID, Batt RD: Total body water volumes for adult males and females estimated from simple anthropometric measurements. *Am J Clin Nutr* 33: 27–39, 1980
8. Waki M, Kral JG, Mazariegos M, Wang J, Pierson RN Jr, Heymsfield SB: Relative expansion of extracellular fluid in obese vs. nonobese women. *Am J Physiol* 261: E199–E203, 1991
9. Silva AM, Heymsfield SB, Gallagher D, Albu J, Pi-Sunyer XF, Pierson RN Jr, Wang J, Heshka S, Sardinha LB, Wang Z: Evaluation of between-methods agreement of extracellular water measurements in adults and children. *Am J Clin Nutr* 88: 315–323, 2008
10. Wang J, Pierson RN Jr: Disparate hydration of adipose and lean tissue require a new model for body water distribution in man. *J Nutr* 106: 1687–1693, 1976
11. Gamble JL Jr, Robertson JS, Hannigan CA, Foster CG, Farr LE: Chloride, bromide, sodium, and sucrose spaces in man. *J Clin Invest* 32: 483–489, 1953
12. Nichols G Jr, Nichols N, Weil WB, Wallace WM: The direct measurement of the extracellular phase of tissues. *J Clin Invest* 32: 1299–1308, 1953
13. Swan RC, Madisso H, Pitts RF: Measurement of extracellular fluid volume in nephrectomized dogs. *J Clin Invest* 33: 1447–1456, 1954
14. Forbes, GB: *Human body composition: Growth, aging, nutrition, and activity*, New York, Springer-Verlag, 1987
15. Cheek DB: Extracellular volume: its structure and measurement and the influence of age and disease. *J Pediatr* 58: 103–125, 1961
16. Basic anatomical and physiological data for use in radiological protection: reference values: A report of age- and gender-related differences in the anatomical and physiological characteristics of reference individuals. ICRP Publication 89. *Ann ICRP* 32: 5–265, 2002
17. International Commission on Radiological Protection. Task Group on Reference Man: *Report of the Task Group on Reference Man: A report*, New York, Pergamon Press, 1975
18. Basic anatomical and physiological data for use in radiological protection: The skeleton. A report of a Task Group of Committee 2 of the International Commission on Radiological Protection. *Ann ICRP* 25: 1–80, 1995
19. Bischoff, E: Einige Gewichts and Trockenbestimmungen der Organe des mensch lichen Korpers. *Zeitsch fu rationelle Medizin* 3: 75, 1863
20. Cooper AR, Forbes RM, Mitchell HH: Further studies on the gross composition and mineral elements of the adult human body. *J Biol Chem* 223: 969–975, 1956
21. Edelman IS, James AH, Baden H, Moore FD: Electrolyte composition of bone and the penetration of radiosodium and deuterium oxide into dog and human bone. *J Clin Invest* 33: 122–131, 1954
22. Forbes GB, Lewis AM: Total sodium, potassium and chloride in adult man. *J Clin Invest* 35: 596–600, 1956
23. Forbes RM, Cooper AR, Mitchell HH: The composition of the adult human body as determined by chemical analysis. *J Biol Chem* 203: 359–366, 1953
24. Clarys JP, Martin AD, Drinkwater DT: Gross tissue weights in the human body by cadaver dissection. *Hum Biol* 56: 459–473, 1984
25. Robinson, RA: Chemical Analysis and Electron Microscopy of Bone. In: *Bone as a Tissue*, edited by Rodahl K, Nicholson, JT, Brown, EM, Philadelphia, McGraw-Hill, 1960, pp. 186–251
26. Michelsen K: Determination in inulin, albumin and erythrocyte spaces in the bone marrow of rabbits. *Acta Physiol Scand* 77: 28–35, 1969
27. Aukland K, Nicolaysen G: Interstitial fluid volume: Local regulatory mechanisms. *Physiol Rev* 61: 556–643, 1981
28. Strange K: Cellular volume homeostasis. *Adv Physiol Educ* 28: 155–159, 2004
29. Stein WD: Cell volume homeostasis: Ionic and nonionic mechanisms.

The sodium pump in the emergence of animal cells. *Int Rev Cytol* 215: 231–258, 2002
30. Willis JS: The balancing act of the naked cell: A brief history of membrane regulation of animal cell volume before 1978. *Adv Exp Med Biol* 559: 1–9, 2004
31. Blandamer MJ, Engberts JB, Gleeson PT, Reis JC: Activity of water in aqueous systems: A frequently neglected property. *Chem Soc Rev* 34: 440–458, 2005
32. Elliott JA, Prickett RC, Elmoazzen HY, Porter KR, McGann LE: A multisolute osmotic virial equation for solutions of interest in biology. *J Phys Chem B* 111: 1775–1785, 2007
33. Essig A, Caplan SR: The use of linear nonequilibrium thermodynamics in the study of renal physiology. *Am J Physiol* 236: F211–F219, 1979
34. Staverman AJ: The theory of measurement of osmotic pressure. *Recueil des Travaux Chimiques des Pays-Bas* 70: 344–352, 1951
35. Essig A, Caplan SR: Water movement: Does thermodynamic interpretation distort reality? *Am J Physiol* 256: C694–C698, 1989
36. Kedem O, Katchalsky A: Thermodynamic analysis of the permeability of biological membranes to non-electrolytes. *Biochim Biophys Acta* 27: 229–246, 1958
37. Kedem O, Katchalsky A: A physical interpretation of the phenomenological coefficients of membrane permeability. *J Gen Physiol* 45: 143–179, 1961
38. Meyer MM, Verkman AS: Human platelet osmotic water and nonelectrolyte transport. *Am J Physiol* 251: C549–C557, 1986
39. Chou CL, Sands JM, Nonoguchi H, Knepper MA: Urea gradient-associated fluid absorption with sigma urea = 1 in rat terminal collecting duct. *Am J Physiol* 258: F1173–F1180, 1990
40. Sands JM, Knepper MA: Urea permeability of mammalian inner medullary collecting duct system and papillary surface epithelium. *J Clin Invest* 79: 138–147, 1987
41. Cass A, Finkelstein A: Water permeability of thin lipid membranes. *J Gen Physiol* 50: 1765–1784, 1967
42. Ly HV, Longo ML: The influence of short-chain alcohols on interfacial tension, mechanical properties, area/molecule, and permeability of fluid lipid bilayers. *Biophys J* 87: 1013–1033, 2004
43. Sands JM: Urea transport: It's not just "freely diffusible" anymore. *News Physiol Sci* 14: 46–47, 1999
44. Curry FE, Michel CC, Mason JC: Osmotic reflection coefficients of capillary walls to low molecular weight hydrophilic solutes measured in single perfused capillaries of the frog mesentery. *J Physiol* 261: 319–336, 1976
45. Landis EM, Pappenheimer, JR: Exchange of substances through the capillary walls. In: *Handbook of Physiology: Section 2: Circulation, Volume 2*, edited by Hamilton WF, Dow P, Washington DC, American Physiological Society, Williams & Wilkins, 1963
46. Vargas F, Johnson JA: Permeability of rabbit heart capillaries to nonelectrolytes. *Am J Physiol* 213: 87–93, 1967
47. Crone C: The permeability of brain capillaries to non-electrolytes. *Acta Physiol Scand* 64: 407–417, 1965
48. Fenstermacher JD, Johnson JA: Filtration and reflection coefficients of the rabbit blood-brain barrier. *Am J Physiol* 211: 341–346, 1966
49. Silver SM, Sterns RH, Halperin ML: Brain swelling after dialysis: Old urea or new osmoles? *Am J Kidney Dis* 28: 1–13, 1996
50. Wolf MB, Watson PD: Measurement of osmotic reflection coefficient for small molecules in cat hindlimbs. *Am J Physiol* 256: H282–H290, 1989
51. Sweeney TE, Beuchat CA: Limitations of methods of osmometry: Measuring the osmolality of biological fluids. *Am J Physiol* 264: R469–R480, 1993
52. Overbeek JT: The Donnan equilibrium. *Prog Biophys Biophys Chem* 6: 57–84, 1956
53. Adair GS, Robinson ME: The analysis of the osmotic pressures of the serum proteins, and the molecular weights of albumins and globulins. *Biochem J* 24: 1864–1889, 1930
54. Nitta S, Ohnuki T, Ohkuda K, Nakada T, Staub NC: The corrected protein equation to estimate plasma colloid osmotic pressure and its development on a nomogram. *Tohoku J Exp Med* 135: 43–49, 1981
55. Scatchard G, Batchelder AC, Brown A: Chemical, clinical, and immunological studies on the products of human plasma fractionation: VI. The osmotic pressure of plasma and of serum albumin. *J Clin Invest* 23: 458–464, 1944
56. Ahlqvist J: Equation for osmotic pressure of serum protein (fractions). *J Appl Physiol* 96: 762–764, 2004
57. Ott H: [Calculation of the colloidal osmotic serum pressure from the protein spectrum, and the average molecular weight of serum protein fractions]. *Klin Wochenschr* 34: 1079–1083, 1956
58. Kallee E: Bennhold's analbuminemia: A follow-up study of the first two cases (1953–1992). *J Lab Clin Med* 127: 470–480, 1996
59. Koot BG, Houwen R, Pot DJ, Nauta J: Congenital analbuminaemia: Biochemical and clinical implications. A case report and literature review. *Eur J Pediatr* 163: 664–670, 2004
60. Nagase S, Shimamune K, Shumiya S: Albumin-deficient rat mutant. *Science* 205: 590–591, 1979
61. Kaysen GA: Plasma composition in the nephrotic syndrome. *Am J Nephrol* 13: 347–359, 1993
62. Vavricka SR, Burri E, Beglinger C, Degen L, Manz M: Serum protein electrophoresis: An underused but very useful test. *Digestion* 79: 203–210, 2009
63. Barclay SA, Bennett D: The direct measurement of plasma colloid osmotic pressure is superior to colloid osmotic pressure derived from albumin or total protein. *Intensive Care Med* 13: 114–118, 1987
64. Friedman AN, Fadem SZ: Reassessment of albumin as a nutritional marker in kidney disease. *J Am Soc Nephrol* 21: 223–230, 2010
65. Gennari FJ: Current concepts: Serum osmolality. Uses and limitations. *N Engl J Med* 310: 102–105, 1984
66. Mange K, Matsuura D, Cizman B, Soto H, Ziyadeh FN, Goldfarb S, Neilson EG: Language guiding therapy: The case of dehydration versus volume depletion. *Ann Intern Med* 127: 848–853, 1997
67. Oster JR, Singer I: Hyponatremia, hyposmolality, and hypotonicity: Tables and fables. *Arch Intern Med* 159: 333–336, 1999
68. Orlov SN, Hamet P: Intracellular monovalent ions as second messengers. *J Membr Biol* 210: 161–172, 2006
69. Leaf A: On the mechanism of fluid exchange of tissues in vitro. *Biochem J* 62: 241–248, 1956
70. Kurbel S: Are extracellular osmolality and sodium concentration determined by Donnan effects of intracellular protein charges and of pumped sodium? *J Theor Biol* 252: 769–772, 2008
71. Macknight AD, Leaf A: Regulation of cellular volume. *Physiol Rev* 57: 510–573, 1977
72. Boddy K, Brown JJ, Davies DL, Elliott A, Harvey I, Haywood JK, Holloway I, Lever AF, Robertson JI, Williams ED: Concurrent estimation of total body and exchangeable body sodium in hypertension. *Clin Sci Mol Med* 54: 187–191, 1978
73. Chamberlain MJ, Fremlin JH, Peters DK, Philip H: Total body sodium by whole body neutron activation in the living subject: Further evidence for non-exchangeable sodium pool. *BMJ* 2: 583–585, 1968
74. Edelman IS, James AH, Brooks L, Moore FD: Body sodium and potassium: IV. The normal total exchangeable sodium: Its measurement and magnitude. *Metabolism* 3: 530–538, 1954
75. Corsa L Jr, Olney JM Jr, Steenburg RW, Ball MR, Moore FD: The measurement of exchangeable potassium in man by isotope dilution. *J Clin Invest* 29: 1280–1295, 1950
76. Muldowney FP, Crooks J, Bluhm MM: The relationship of total exchangeable potassium and chloride to lean body mass, red cell mass and creatinine excretion in man. *J Clin Invest* 36: 1375–1381, 1957
77. Schrier RW: Decreased effective blood volume in edematous disorders: What does this mean? *J Am Soc Nephrol* 18: 2028–2031, 2007
78. Gauer OH, Henry JP, Behn C: The regulation of extracellular fluid volume. *Annu Rev Physiol* 32: 547–595, 1970

79. Hollenberg NK: Set point for sodium homeostasis: Surfeit, deficit, and their implications. *Kidney Int* 17: 423–429, 1980
80. Manning RD Jr, Guyton AC: Control of blood volume. *Rev Physiol Biochem Pharmacol* 93: 70–114, 1982
81. Aukland K, Reed RK: Interstitial-lymphatic mechanisms in the control of extracellular fluid volume. *Physiol Rev* 73: 1–78, 1993
82. Renkin EM: Some consequences of capillary permeability to macromolecules: Starling's hypothesis reconsidered. *Am J Physiol* 250: H706–H710, 1986
83. Starling, EH: On the absorption of fluids from the connective tissue spaces. *J Physiol* 19: 312–326, 1896
84. Levick JR, Michel CC: Microvascular fluid exchange and the revised Starling principle. *Cardiovasc Res* 87: 198–210, 2010
85. Lai WM, Hou JS, Mow VC: A triphasic theory for the swelling and deformation behaviors of articular cartilage. *J Biomech Eng* 113: 245–258, 1991
86. Maroudas A: Distribution and diffusion of solutes in articular cartilage. *Biophys J* 10: 365–379, 1970
87. Aukland K, Wiig H, Tenstad O, Renkin EM: Interstitial exclusion of macromolecules studied by graded centrifugation of rat tail tendon. *Am J Physiol* 273: H2794–H2803, 1997
88. Reed RK, Lepsoe S, Wiig H: Interstitial exclusion of albumin in rat dermis and subcutis in over- and dehydration. *Am J Physiol* 257: H1819–H1827, 1989
89. Maroudas A, Bannon C: Measurement of swelling pressure in cartilage and comparison with the osmotic pressure of constituent proteoglycans. *Biorheology* 18: 619–632, 1981
90. Meyer FA: Macromolecular basis of globular protein exclusion and of swelling pressure in loose connective tissue (umbilical cord). *Biochim Biophys Acta* 755: 388–399, 1983
91. Maroudas AI: Balance between swelling pressure and collagen tension in normal and degenerate cartilage. *Nature* 260: 808–809, 1976
92. Iozzo RV: Matrix proteoglycans: From molecular design to cellular function. *Annu Rev Biochem* 67: 609–652, 1998
93. Brace RA, Guyton AC: Interstitial fluid pressure: Capsule, free fluid, gel fluid, and gel absorption pressure in subcutaneous tissue. *Microvasc Res* 18: 217–228, 1979
94. Brace RA: Progress toward resolving the controversy of positive vs. negative interstitial fluid pressure. *Circ Res* 49: 281–297, 1981
95. Gyenge CC, Tenstad O, Wiig H: In vivo determination of steric and electrostatic exclusion of albumin in rat skin and skeletal muscle. *J Physiol* 552: 907–916, 2003
96. Levick JR: Capillary filtration-absorption balance reconsidered in light of dynamic extravascular factors. *Exp Physiol* 76: 825–857, 1991
97. Rippe B, Haraldsson B: Transport of macromolecules across microvascular walls: The two-pore theory. *Physiol Rev* 74: 163–219, 1994
98. Adamson RH, Lenz JF, Zhang X, Adamson GN, Weinbaum S, Curry FE: Oncotic pressures opposing filtration across non-fenestrated rat microvessels. *J Physiol* 557: 889–907, 2004
99. Hu X, Adamson RH, Liu B, Curry FE, Weinbaum S: Starling forces that oppose filtration after tissue oncotic pressure is increased. *Am J Physiol Heart Circ Physiol* 279: H1724–H1736, 2000
100. Drake RE, Dhother S, Teague RA, Gabel JC: Protein osmotic pressure gradients and microvascular reflection coefficients. *Am J Physiol* 273: H997–H1002, 1997
101. Weinbaum S, Tarbell JM, Damiano ER: The structure and function of the endothelial glycocalyx layer. *Annu Rev Biomed Eng* 9: 121–167, 2007
102. Guyton AC: A concept of negative interstitial pressure based on pressures in implanted perforated capsules. *Circ Res* 12: 399–414, 1963
103. Guyton AC, Granger HJ, Taylor AE: Interstitial fluid pressure. *Physiol Rev* 51: 527–563, 1971
104. Guyton AC: Interstitial fluid presure: II. Pressure-volume curves of interstitial space. *Circ Res* 16: 452–460, 1965
105. Wiig H, Reed RK: Compliance of the interstitial space in rats: II. Studies on skin. *Acta Physiol Scand* 113: 307–315, 1981
106. Pozzi A, Zent R: Integrins: Sensors of extracellular matrix and modulators of cell function. *Nephron Exp Nephrol* 94: e77–84, 2003
107. Reed RK, Rubin K: Transcapillary exchange: Role and importance of the interstitial fluid pressure and the extracellular matrix. *Cardiovasc Res* 87: 211–217, 2010
108. Berg A, Rubin K, Reed RK: Cytochalasin D induces edema formation and lowering of interstitial fluid pressure in rat dermis. *Am J Physiol Heart Circ Physiol* 281: H7–H13, 2001
109. Lund T, Onarheim H, Wiig H, Reed RK: Mechanisms behind increased dermal imbibition pressure in acute burn edema. *Am J Physiol* 256: H940–H948, 1989
110. Reed RK, Rubin K, Wiig H, Rodt SA: Blockade of beta 1-integrins in skin causes edema through lowering of interstitial fluid pressure. *Circ Res* 71: 978–983, 1992
111. Lund T, Wiig H, Reed RK: Acute postburn edema: Role of strongly negative interstitial fluid pressure. *Am J Physiol* 255: H1069–H1074, 1988
112. Reed RK, Rodt SA: Increased negativity of interstitial fluid pressure during the onset stage of inflammatory edema in rat skin. *Am J Physiol* 260: H1985–H1991, 1991
113. Heir S, Wiig H: Subcutaneous interstitial fluid colloid osmotic pressure in dehydrated rats. *Acta Physiol Scand* 133: 365–371, 1988
114. Moore FD: The effects of hemorrhage on body composition. *N Engl J Med* 273: 567–577, 1965
115. Alper CA: Plasma protein measurements as a diagnostic aid. *N Engl J Med* 291: 287–290, 1974
116. Armstrong SH Jr, Kark RM, Schoenberger JA, Shatkin J, Sights R: Colloid osmotic pressures of serum proteins in nephrosis and cirrhosis: Relations to electrophoretic distributions and average molecular weights. *J Clin Invest* 33: 297–310, 1954
117. Fadnes HO, Pape JF, Sundsfjord JA: A study on oedema mechanism in nephrotic syndrome. *Scand J Clin Lab Invest* 46: 533–538, 1986
118. Koomans HA, Geers AB, Dorhout Mees EJ, Kortlandt W: Lowered tissue-fluid oncotic pressure protects the blood volume in the nephrotic syndrome. *Nephron* 42: 317–322, 1986
119. Canaan-Kuhl S, Venkatraman ES, Ernst SI, Olshen RA, Myers BD: Relationships among protein and albumin concentrations and oncotic pressure in nephrotic plasma. *Am J Physiol* 264: F1052–F1059, 1993
120. Theuns-Valks SD, van Wijk JA, van Heerde M, Dolman KM, Bokenkamp A: Abdominal pain and vomiting in a boy with nephrotic syndrome. *Clin Pediatr* 50: 470–473, 2011
121. Van de Walle JG, Donckerwolcke RA, Greidanus TB, Joles JA, Koomans HA: Renal sodium handling in children with nephrotic relapse: Relation to hypovolaemic symptoms. *Nephrol Dial Transplant* 11: 2202–2208, 1996
122. Wang SJ, Tsau YK, Lu FL, Chen CH: Hypovolemia and hypovolemic shock in children with nephrotic syndrome. *Acta Paediatr Taiwan* 41: 179–183, 2000
123. Bernard DB, Alexander EA, Couser WG, Levinsky NG: Renal sodium retention during volume expansion in experimental nephrotic syndrome. *Kidney Int* 14: 478–485, 1978
124. Ichikawa I, Rennke HG, Hoyer JR, Badr KF, Schor N, Troy JL, Lechene CP, Brenner BM: Role for intrarenal mechanisms in the impaired salt excretion of experimental nephrotic syndrome. *J Clin Invest* 71: 91–103, 1983
125. Svenningsen P, Bistrup C, Friis UG, Bertog M, Haerteis S, Krueger B, Stubbe J, Jensen ON, Thiesson HC, Uhrenholt TR, Jespersen B, Jensen BL, Korbmacher C, Skott O: Plasmin in nephrotic urine activates the epithelial sodium channel. *J Am Soc Nephrol* 20: 299–310, 2009
126. Vande Walle JG, Donckerwolcke RA, van Isselt JW, Derkx FH, Joles JA, Koomans HA: Volume regulation in children with early relapse of

minimal-change nephrosis with or without hypovolaemic symptoms. *Lancet* 346: 148–152, 1995
127. Palmer BF, Alpern RJ: Pathogenesis of edema formation in the nephrotic syndrome. *Kidney Int Suppl* 59: S21–S27, 1997
128. Schrier RW, Fassett RG: A critique of the overfill hypothesis of sodium and water retention in the nephrotic syndrome. *Kidney Int* 53: 1111–1117, 1998
129. Rostoker G, Behar A, Lagrue G: Vascular hyperpermeability in nephrotic edema. *Nephron* 85: 194–200, 2000
130. Koomans, HA: Pathophysiology of oedema in idiopathic nephrotic syndrome. *Nephrol Dial Transplant* 18[Suppl 6]: vi30–vi32, 2003
131. Vande Walle JG, Donckerwolcke RA, Koomans HA: Pathophysiology of edema formation in children with nephrotic syndrome not due to minimal change disease. *J Am Soc Nephrol* 10: 323–331, 1999
132. Appelboom JW, Brodsky WA, Tuttle WS, Diamond I: The freezing point depression of mammalian tissues after sudden heating in boiling distilled water. *J Gen Physiol* 41: 1153–1169, 1958
133. Maffly RH, Leaf A: The potential of water in mammalian tissues. *J Gen Physiol* 42: 1257–1275, 1959
134. Hillier TA, Abbott RD, Barrett EJ: Hyponatremia: Evaluating the correction factor for hyperglycemia. *Am J Med* 106: 399–403, 1999
135. Moran SM, Jamison RL: The variable hyponatremic response to hyperglycemia. *West J Med* 142: 49–53, 1985
136. Tzamaloukas AH, Ing TS, Siamopoulos KC, Rohrscheib M, Elisaf MS, Raj DS, Murata GH: Body fluid abnormalities in severe hyperglycemia in patients on chronic dialysis: Theoretical analysis. *J Diabetes Complications* 21: 374–380, 2007
137. Nguyen MK, Kurtz I: Is the osmotically inactive sodium storage pool fixed or variable? *J Appl Physiol* 102: 445–447, 2007
138. Basser PJ, Schneiderman R, Bank RA, Wachtel E, Maroudas A: Mechanical properties of the collagen network in human articular cartilage as measured by osmotic stress technique. *Arch Biochem Biophys* 351: 207–219, 1998
139. Farber SJ, Soberman RJ: Total body water and total exchangeable sodium in edematous states due to cardiac, renal or hepatic disease. *J Clin Invest* 35: 779–791, 1956
140. Heer M, Baisch F, Kropp J, Gerzer R, Drummer C: High dietary sodium chloride consumption may not induce body fluid retention in humans. *Am J Physiol Renal Physiol* 278: F585–F595, 2000
141. Kaye M: An investigation into the cause of hyponatremia in the syndrome of inappropriate secretion of antidiuretic hormone. *Am J Med* 41: 910–926, 1966
142. Palacios C, Wigertz K, Martin BR, Jackman L, Pratt JH, Peacock M, McCabe G, Weaver CM: Sodium retention in black and white female adolescents in response to salt intake. *J Clin Endocrinol Metab* 89: 1858–1863, 2004
143. Schwartz WB, Bennett W, Curelop S, Bartter FC: A syndrome of renal sodium loss and hyponatremia probably resulting from inappropriate secretion of antidiuretic hormone. *Am J Med* 23: 529–542, 1957
144. Clift GV, Schletter FE, Moses AM, Streeten DH: Syndrome of inappropriate vasopressin secretion: Studies on the mechanism of the hyponatremia in a patient. *Arch Intern Med* 118: 453–460, 1966
145. Deming Q, Gerbode F: Observations on sodium balance in patients undergoing mitral valvotomy. *Surg Forum* 4: 18–22, 1953
146. Roos JC, Koomans HA, Dorhout Mees EJ, Delawi IM: Renal sodium handling in normal humans subjected to low, normal, and extremely high sodium supplies. *Am J Physiol* 249: F941–F947, 1985
147. Seeliger E, Ladwig M, Reinhardt HW: Are large amounts of sodium stored in an osmotically inactive form during sodium retention? Balance studies in freely moving dogs. *Am J Physiol Regul Integr Comp Physiol* 290: R1429–R1435, 2006
148. Wilson GM, Edelman IS, Brooks L, Myrden JA, Harken DE, Moore FD: Metabolic changes associated with mitral valvuloplasty. *Circulation* 9: 199–219, 1954
149. Wynn V: The osmotic behaviour of the body cells in man: Significance of changes of plasma-electrolyte levels in body-fluid disorders. *Lancet* 273: 1212–1218, 1957
150. Heer M, Frings-Meuthen P, Titze J, Boschmann M, Frisch S, Baecker N, Beck L: Increasing sodium intake from a previous low or high intake affects water. *Br J Nutr* 101: 1286–1294, 2009
151. Luft FC, Rankin LI, Bloch R, Weyman AE, Willis LR, Murray RH, Grim CE, Weinberger MH: Cardiovascular and humoral responses to extremes of sodium intake in normal black and white men. *Circulation* 60: 697–706, 1979
152. Nolph KD, Schrier RW: Sodium, potassium and water metabolism in the syndrome of inappropriate antidiuretic hormone secretion. *Am J Med* 49: 534–545, 1970
153. Holbrook JT, Patterson KY, Bodner JE, Douglas LW, Veillon C, Kelsay JL, Mertz W, Smith JC Jr: Sodium and potassium intake and balance in adults consuming self-selected diets. *Am J Clin Nutr* 40: 786–793, 1984
154. Kopple, JD: Uses and limitations of the balance technique. *JPEN J Parenter Enteral Nutr* 11: 79S–85S, 1987
155. Wilson GM, Olney JM, Brooks L, Myrden JA, Ball MR, Moore FD: Body sodium and potassium: II. A comparison of metabolic balance and isotope dilution methods of study. *Metabolism* 3: 324–333, 1954
156. Titze J, Bauer K, Schafflhuber M, Dietsch P, Lang R, Schwind KH, Luft FC, Eckardt KU, Hilgers KF: Internal sodium balance in DOCA-salt rats: A body composition study. *Am J Physiol Renal Physiol* 289: F793–F802, 2005
157. Zolotova VF, Priadeina TE, Archibasova VK, Shterental IS: [Distribution of sodium in the tissues in experimental salt hypertension]. *Kardiologiia* 15: 32–36, 1975
158. Titze J, Krause H, Hecht H, Dietsch P, Rittweger J, Lang R, Kirsch KA, Hilgers KF: Reduced osmotically inactive Na storage capacity and hypertension in the Dahl model. *Am J Physiol Renal Physiol* 283: F134–F141, 2002
159. Machnik A, Neuhofer W, Jantsch J, Dahlmann A, Tammela T, Machura K, Park JK, Beck FX, Muller DN, Derer W, Goss J, Ziomber A, Dietsch P, Wagner H, van Rooijen N, Kurtz A, Hilgers KF, Alitalo K, Eckardt KU, Luft FC, Kerjaschki D, Titze J: Macrophages regulate salt-dependent volume and blood pressure by a vascular endothelial growth factor-C-dependent buffering mechanism. *Nat Med* 15: 545–552, 2009
160. Ivanova LN, Archibasova VK, Shterental I: [Sodium-depositing function of the skin in white rats]. *Fiziol Zh SSSR Im I M Sechenova* 64: 358–363, 1978
161. Titze J, Shakibaei M, Schafflhuber M, Schulze-Tanzil G, Porst M, Schwind KH, Dietsch P, Hilgers KF: Glycosaminoglycan polymerization may enable osmotically inactive Na+ storage in the skin. *Am J Physiol Heart Circ Physiol* 287: H203–H208, 2004
162. Boardman KC, Swartz MA: Interstitial flow as a guide for lymphangiogenesis. *Circ Res* 92: 801–808, 2003
163. Browning JA, Saunders K, Urban JP, Wilkins RJ: The influence and interactions of hydrostatic and osmotic pressures on the intracellular milieu of chondrocytes. *Biorheology* 41: 299–308, 2004
164. Rutkowski JM, Swartz MA: A driving force for change: Interstitial flow as a morphoregulator. *Trends Cell Biol* 17: 44–50, 2007
165. Urban JP, Bayliss MT: Regulation of proteoglycan synthesis rate in cartilage in vitro: Influence of extracellular ionic composition. *Biochim Biophys Acta* 992: 59–65, 1989
166. Maroudas A, Evans H: A study of ionic equilibria in cartilage. *Connective Tissue Research* 1: 69–77, 1972
167. McGee MP, Morykwas M, Levi-Polyachenko N, Argenta L: Swelling and pressure-volume relationships in the dermis measured by osmotic-stress technique. *Am J Physiol Regul Integr Comp Physiol* 296: R1907–R1913, 2009
168. Urban JP: The chondrocyte: A cell under pressure. *Br J Rheumatol* 33: 901–908, 1994

169. Hopewell B, Urban JP: Adaptation of articular chondrocytes to changes in osmolality. *Biorheology* 40: 73–77, 2003
170. Kurtz TW, Al-Bander HA, Morris RC Jr: "Salt-sensitive" essential hypertension in men: Is the sodium ion alone important? *N Engl J Med* 317: 1043–1048, 1987
171. Kurtz TW, Morris RC Jr: Dietary chloride as a determinant of "sodium-dependent" hypertension. *Science* 222: 1139–1141, 1983
172. Luft FC, Zemel MB, Sowers JA, Fineberg NS, Weinberger MH: Sodium bicarbonate and sodium chloride: Effects on blood pressure and electrolyte homeostasis in normal and hypertensive man. *J Hypertens* 8: 663–670, 1990
173. Ziomber A, Machnik A, Dahlmann A, Dietsch P, Beck FX, Wagner H, Hilgers KF, Luft FC, Eckardt KU, Titze J: Sodium-, potassium-, chloride-, and bicarbonate-related effects on blood pressure and electrolyte homeostasis in deoxycorticosterone acetate-treated rats. *Am J Physiol Renal Physiol* 295: F1752–F1763, 2008
174. Green J, Kleeman CR: Role of bone in regulation of systemic acid-base balance. *Kidney Int* 39: 9–26, 1991
175. Neuman WF, Mulryan BJ: Synthetic hydroxyapatite crystals: 3. The carbonate system. *Calcif Tissue Res* 1: 94–104, 1967
176. Nichols N, Nichols G Jr: Effect of large loads of sodium on bone and soft tissue composition. *Proc Soc Exp Biol Med* 96: 835–839, 1957
177. Ivanova LN, Melidi NN, Merjeyevskaya VM, Sterental LS, Zolotova VF: The response to water-salt loading: Sodium metabolism in spontaneously hypertensive rats. *Biomed Biochim Acta* 46: 993–997, 1987
178. Merzhievskaia VM, Shterental I: [Kinetics of tissue sodium metabolism and the vascular reactivity to vasopressor agents in healthy persons with different degree of risk of developing arterial hypertension]. *Kardiologiia* 28: 30–33, 1988
179. Bernstein AM, Willett WC: Trends in 24-h urinary sodium excretion in the United States, 1957–2003: A systematic review. *Am J Clin Nutr* 92: 1172–1180, 2010
180. Brown IJ, Tzoulaki I, Candeias V, Elliott P: Salt intakes around the world: Implications for public health. *Int J Epidemiol* 38: 791–813, 2009
181. McCarron DA, Geerling JC, Kazaks AG, Stern JS: Can dietary sodium intake be modified by public policy? *Clin J Am Soc Nephrol* 4: 1878–1882, 2009
182. Ferrannini E, Smith JD, Cobelli C, Toffolo G, Pilo A, DeFronzo RA: Effect of insulin on the distribution and disposition of glucose in man. *J Clin Invest* 76: 357–364, 1985
183. Forbes GB: Studies on sodium in bone. *J Pediatr* 56: 180–190, 1960
184. Manery JF: Water and electrolyte metabolism. *Physiol Rev* 34: 334–417, 1954
185. Levitt DG: The pharmacokinetics of the interstitial space in humans. *BMC Clin Pharmacol* 3: 3, 2003
186. Gong JK, Arnold JS, Cohn SH: Composition of trabecular and cortical bone. *Anat Rec* 149: 325–331, 1964
187. Gilanyi M, Ikrenyi C, Fekete J, Ikrenyi K, Kovach AG: Ion concentrations in subcutaneous interstitial fluid: Measured versus expected values. *Am J Physiol* 255: F513–F519, 1988

Supplemental information for this article is available online at http://www.jasn.org/.

Supplemental Materials

1. Index of Mathematical Symbols

Symbol	Definition
M_u	Urea mass transfer rate
G_u or R_u	Urea generation or loss rate
$\Delta[C]_u$	Hypothetical urea gradient (transcellular or transcapillary)
PS_{urea}	Permeability * Surface Area product or urea diffusion capacity; calculated for entire surface area of all cell membranes ($PS_{urea\text{-}cm}$) or cerebral capillaries ($PS_{urea\text{-}brain}$)
Π	Osmotic Pressure in mm Hg
MW_{av}	Average molecular weight of a protein or mixture of proteins determined using limiting slope of the osmotic pressure-protein concentration relationship
φ	True osmotic coefficient of a solute
$d\Pi / dc\ (c = 0)$	Slope of the osmotic pressure-protein concentration relationship as protein concentration approaches zero ("limiting slope")
z_{eff}	Effective valence of a salt; for example z_{eff} for NaCl equals 2. Note that z_{eff} for higher order salts is not as easily predicted with significant non-linear behavior.
φ	Effective osmotic coefficient which takes into account counter-ion since it multiplies true osmotic coefficient by effective valence.
φ_{pNa+K}	Effective osmotic coefficient of plasma Na^+ and K^+
φ_{tbNa+K}	Effective osmotic coefficient of total body Na^+ and K^+
φ_{pi}	Effective osmotic coefficient of the "i^{th}" non-Na^+, non-K^+ plasma solute
φ_{tbi}	Effective osmotic coefficient of the "i^{th}" non-Na^+, non-K^+ total body solute
V_{Di}	Volume of distribution as a fraction of TBW of the "i^{th}" non-Na^+, non-K^+ total body solute
φ_{neNa+K}	Effective osmotic coefficient for non-exchangeable total body Na^+ and K^+; essentially equals zero.
φ_{eNa+K}	Effective osmotic coefficient for exchangeable total body Na^+ and K^+.
m_{osm}, $b_{[osm]}$	Slope & y-intercept of the general relationship between plasma and total body osmolality

$Na^+_{ex} + K^+_{ex}$	Radioisotope exchangeable Na^+ plus exchangeable K^+. Typical exchange times are 24 hours for Na^+ and 40-48 hours for K^+.
$Na^+_{eA} + K^+_{eA}$	Excess (or "residual") Na^+ and K^+ which is osmotically active; the latter is defined as an osmotic coefficient approaching φ_{pNa+K}.
$Na^+_{eI} + K^+_{eI}$	Excess (or "residual") Na^+ and K^+ which is osmotically inactive with an osmotic coefficient of near zero.
f_{PW}	Plasma water fraction – usually about 0.93 but may fall with hyperproteinemia or hyperlipidemia. Allows one to convert molar concentrations to molal concentrations: Molal concentration * f_{PW} = Molar Concentration
$[S]_i$	Plasma molar concentration of the "i^{th}" non-Na^+, non-K^+ solute.
TB $[s]_i$	Total body molal concentration of the "i^{th}" non-Na^+, non-K^+ solute.
G_{Na}	Corrects plasma $[Na^+]$ for hyperglycemia related translocational hyponatremia. Proposed to range from 1.5 – 2.4 mEq/L fall in plasma $[Na^+]$ per 100 mg/dL rise in plasma glucose.
$[Na^+]_{GAG}$ $[Cl^-]_{GAG}$	Na^+ and Cl^- concentrations in the interstitial GAG phase of the three phase model.
$[Na^+]_{if}$ $[Cl^-]_{if}$	Na^+ and Cl^- concentrations in the interstitial "free fluid" phase of the three phase model.
FCD	Fixed charge density – concentration of interstitial GAG negative charge

2. Anthropomorphic Equations for TBW

Watson et al.:[1]
Males: 0.1074 * Height + 0.3362 * Weight – 0.09516 * Age + 2.447
Females: 0.1069 * Height + 0.2466 * Weight – 2.097

Chumlea et al.:[2]
Caucasian Males: -0.62 * BMI + 0.5 * Weight – 0.03 * Age – 23.04
Caucasian Females: 0.18 * Height + 0.2 * Weight – 0.01 * Age – 10.5
African American Males: 0.25 * Height + 0.34 * Weight – 0.09 * Age – 18.37
African American Females: 0.24 * Height + 0.22 * Weight – 0.05 * Age – 16.71

Ellis:[3]
Males: 0.284 * Height + 0.25 * Weight – 0.092 * Age – 21.9
Females: 0.273 * Height + 0.17 * Weight – 0.045 * Age – 21.9
Units: TBW in liters, Height in cm, Weight in kg, Age in years, and BMI in kg/m^2

3. Qualitative Calculation of Hypothetical Urea Gradients

These calculations are designed only to qualitatively illustrate underlying physiologic principles. We assume no renal excretion or extrarenal metabolism of urea as a simplification. To calculate a potential urea concentration gradient ($\Delta[C]_u$), we equate urea generation rate (G_u) to total urea mass transfer rate (M_u) and solve for $\Delta[C]_u$:

$$M_u = PS_{urea\text{-}cm} * \Delta[C]_u = G_u$$

$$\Delta[C]_u = G_u \div PS_{urea\text{-}cm}$$

where $PS_{urea\text{-}cm}$ equals the cell membrane diffusive capacity for urea. To calculate $PS_{urea\text{-}cm}$ area, we use the average urea permeability coefficient for artificial lipid bilayers ($P_D \sim 3 \times 10^{-6}$ cm/s) and envision an average human spherical cell with a radius of 10 μm and assume that there are 10^{13} cells in an average adult human:[4-6]

$$PS_{urea\text{-}cm} = 3 \times 10^{-6} \text{ cm/s} * 4 * \Pi * (0.001 \text{ cm})^2 * 10^{13} = 22.6 \text{ L/min}$$

Based on literature estimates for G_u in normal subjects, $\Delta[C]_u$ can be calculated as follows:[7, 8]

$$G_u = 0.5 \text{ mmol/min } (\sim 40 \text{ g urea/day})$$

$$\Delta[C]_u = 0.46 \text{ mmol/min} \div 22.6 \text{ L/min}$$

$$\Delta[C]_u \cong 0.025 \text{ mM}$$

In essence, the very large cell surface area ($\sim 1.25 \times 10^8$ cm^2 or 12,500 m^2) minimizes transcellular urea gradients despite low permeability (P_D). A similar approach can be taken to calculate a cerebral transcapillary urea gradient during high efficiency hemodialysis as BUN falls at a rate of 50 mg/dL/hour which equals a blood [urea] rate (ΔBlood [urea]) of 17.8 mM/h. A total urea mass removal rate, R_u, from cerebral blood is first calculated:

$$R_u = CBV * \Delta\text{Blood [urea]}$$

$$CBV = 0.063\text{L}$$

$$R_u = 0.019 \text{ mmol/min}$$

where CBV is cerebral blood volume.[9] To delineate transcapillary urea mass transfer rate, total brain urea

capillary diffusion capacity ($PS_{urea\text{-}brain}$) is used to obtain a potential transcapillary urea concentration gradient:[10]

$$PS_{urea\text{-}brain} \cong 75 \text{ mL/min}$$

$$\Delta[C]_u = R_u \div PS_{urea\text{-}brain}$$

$$\Delta[C]_u = 0.019 \text{ mmol/min} \div 0.08 \text{ L/min} \cong 0.25 \text{ mM}$$

4. Average Plasma Protein Molecular Weight in Low Albumin States

Average protein molecular weight (MW_{av}) may be calculated from the relationship between protein osmotic pressure and concentration:

$$\Pi\ (37^oC;\ mm\ Hg) = 19.34 * \varphi * [c]$$

$$\Pi\ (37^oC;\ mm\ Hg) = (19.34 * \varphi * 10 * c) \div (MW_{av} * f_W)$$

where φ is the osmotic coefficient (see above), [c] is molal protein concentration, f_W is the fraction of water in the solution, and c is concentration in g/dL. As protein concentration approaches zero, φ and f_W approach 1, and the limiting slope ($^{d_\pi}/_{dc}$) of the relationship provides MW_{av}:

$$MW_{av} \text{ (in kD)} = 193.4 \div {}^{d_\pi}/_{dc}\ (c = 0)$$

As a first approximation, MW_{av} provides an estimate of osmotic efficiency with lower molecular weight proteins generating greater osmotic pressure per g/dL of protein. Higher order osmotic virial coefficients (see above) may alter the MW_{av} osmotic efficiency relationship particularly at higher protein concentrations, but the MW_{av} concept is qualitatively useful to illustrate determinants of plasma COP. More importantly, MW_{av} of protein mixtures ($MW_{av\text{-}mix}$) may be calculated as follows:[11]

$$\frac{1}{MW_{av\text{-}mix}} = \Sigma \frac{f_i}{MW_{av\text{-}i}}$$

where f_i is the fraction of the i^{th} protein component and $MW_{av\text{-}i}$ the average MW of that component. Using this relationship and literature estimates, plasma protein average molecular weight may be calculated in various

conditions (Supplemental Table 1).[11-16 13, 17, 18]

5. Plasma Tonicity to Total Body Tonicity Relationship

The osmotic coefficient φ relates solute concentration to osmotic pressure Π for non-dilute solutions:

$$\Pi\ (37^{o}C;\ mm\ Hg) = 19.34 * \varphi * z * [c]$$

where [c] represents molal solute concentration and z is valence for electrolyte solutes. While φ is often denoted as a constant, it actually is a polynomial function of molal solute concentration:[19]

$$\varphi = 1 + \varphi_1 * [c] + \varphi_2 [c]^2 + \varphi_3 [c]^3 + \ldots.$$

where φ_1, φ_2, and φ_3 are osmotic virial coefficients of any value including less than zero. As [c] approaches zero (increasingly dilute solution), the higher order terms become inconsequential and φ first approaches $1 + \varphi_1$ and then approaches the ideal value of 1. Most salts at physiologic concentrations are aptly described by $1 + \varphi_1$; thus osmotic pressure may be expressed as a function of a constant osmotic coefficient. However, body fluids are mixtures of solutes including proteins with complex osmotic behavior. A composite osmotic coefficient φ_c may be defined for a solution with n solutes:

$$\Pi\ (37^{o}C;\ mm\ Hg) = 19.34 * \varphi_c * \mathbf{\Sigma}\ z_i * [c]_i$$

Analogous to single solute solutions, φ_c is not constant but a complex function of each solute concentration with interaction terms between solutes.[19] For example, φ_c for plasma will vary with plasma $[Na^+]$, glucose, and other solute concentrations. At the limited physiologically relevant solute concentrations, we assume minimal interaction between solutes and express the osmotic pressure of the mixed solution as the sum of its component osmotic pressures:[20-23]

$$\Pi\ (37^{o}C;\ mm\ Hg) = 19.34 * \mathbf{\Sigma}\ z_i * \varphi_i * [c]_i$$

$$\varphi_c = (\mathbf{\Sigma}\ z_i * \varphi_i * [c]_i) \div (\Sigma\ z_i * [c]_i)$$

Experimentally, individual osmotic coefficients may be obtained by measuring the change in osmolality with addition of a given solute to the body fluid, while other solute concentrations are held relatively constant.[24, 25] Since body cation salts have many counterions (chloride, bicarbonate, phosphate, albumin, intracellular proteins, etc.), an effective valence (z_{eff}) and osmotic coefficient (φ) will be used throughout:

$$\varphi_{cation} = \varphi_{cation} * z_{eff}$$

With this construct, expressions for plasma and total body osmolality may be derived:

$$\text{Plasma [c]} = \text{Plasma [C]} \div f_{PW}$$

$$P_{osm} = \varphi_{pNa+K} * P_{Na+K} / f_{PW} + \Sigma\ \varphi_{pi} * \text{Plasma } [S]_i/f_{PW}$$

$$\text{Total Body [c]} = \text{TB C} \div \text{TBW}$$

$$\varphi_{tb} = \varphi_{tb} * z_{eff\text{-}tb}$$

$$TB_{osm} = \varphi_{tbNa+K} * \frac{\text{TB } Na^+ + \text{TB } K^+}{\text{TBW}} + \Sigma\ \varphi_{tbi} * \frac{\text{TB } S_i}{\text{TBW}}$$

where [c] and [C] represent molal and molar concentrations respectively, f_{PW} is the plasma water fraction (normally ~ 0.93), φ_{pNa+K} is the effective osmotic coefficient for plasma Na^+ and K^+ salts, and φ_{tbNa+K} is the effective osmotic coefficient for total body Na^+ and K^+ salts. Note that φ_{pNa+K} and φ_{tbNa+K} both account for Na^+ and K^+ as well as their accompanying anions with the inclusion of effective valence (z_{eff}). S represents "n" non-Na^+ and K^+ cation salts and uncharged substances, which are multiplied by their respective osmotic coefficients and summed (Σ). Plasma non-Na^+ and K^+ solutes may be related to total body solute content (TB S) using the solute volume of distribution (V_D) expressed *as a fraction of TBW*:

$$\text{Plasma } [S]_i = \frac{f_{PW}}{V_{Di}} * \text{TB } [s]_i$$

Total body Na^+ and K^+ is divided into non-exchangeable ($Na^+_{ne} + K^+_{ne}$) and exchangeable ($Na^+_{ex} + K^+_{ex}$) fractions:

$$TB\ Na^+ + TB\ K^+ = (Na^+_{ne} + K^+_{ne}) + (Na^+_{ex} + K^+_{ex})$$

$$\varphi_{tbNa+K} * \frac{TB\ Na^+ + TB\ K^+}{TBW} = \varphi_{neNa+K} * \frac{Na^+_{ne} + K^+_{ne}}{TBW} + \varphi_{eNa+K} * \frac{Na^+_{ex} + K^+_{ex}}{TBW}$$

Non-exchangeable Na^+ and K^+ do not affect body water distribution; thus $\varphi_{neNa+K} = 0$ and total body Na^+ and K^+ osmolality equals exchangeable Na^+ and K^+ osmolality.

Plasma and total body osmolality may differ. We relate P_{osm} and TB_{osm} as a linear relationship over the limited physiologic range of osmolality:

$$P_{osm} = m_{osm} * TB_{osm} + b_{[osm]}$$

Using the relationship between P_{osm} and TB_{osm}, we can derive a relationship for P_{Na}:

$$P_{Na} = \frac{f_{PW} * m_{osm}}{\varphi_{pNa+K}} \left(\frac{\varphi_{eNa+K} * Na^+_{ex} + K^+_{ex}}{TBW} + \sum TB\ [s]_i * (\varphi_{tbi} - \varphi_{pi}/V_{Di}) \right) + \frac{f_{PW} * b_{[osm]}}{\varphi_{pNa+K}} - P_K$$

The summation term of non-Na^+ and K^+ solutes allows one to delineate effective and ineffective osmoles and their effect on P_{Na}. Assuming minimal differences in plasma and total body osmotic coefficients ($\varphi_{tbi} \cong \varphi_{pi}$), if the solute distributes throughout TBW with $V_{Di} \cong 1$, then the solute concentration is equal in all body compartments and changes in body solute content do not affect P_{Na}; the solute behaves as an ineffective osmole. Urea and ethanol permeate into all body water compartments, distribute into TBW, and do not affect P_{Na}. Plasma solutes residing in the ECF such as glucose or mannitol exhibit $V_D < 1$ and lower P_{Na} since $\varphi_{tbGlucose} - (\varphi_{pGlucose} / V_{DGlucose})$ is less than zero. Conversely, solutes with higher tissue concentrations compared to plasma have a $V_D > 1$ and raise P_{Na} as $\varphi_{tbSi} - (\varphi_{pSi}/V_{DSi}) > 0$. Intuitively, intracellular solutes draw water into cells raising P_{Na}, while extracellular solutes tend to pull water into the ECF lowering P_{Na}.

To incorporate exchangeable, excess Na^+ and K^+ into the P_{Na} relationship, exchangeable Na^+ and K^+

may be modeled as two components; one iso-osmolar to plasma Na^+ and K^+ distributed across TBW and another representing excess Na^+ and K^+ distributed across TBW and divided into osmotically active and inactive components. The osmotically active component ($Na^+_{eA} + K^+_{eA}$) is assumed to have an osmotic coefficient equal to or near φ_{pNa+K}, while the inactive component ($Na^+_{eI} + K^+_{eI}$) is assumed to have a coefficient equal to zero (or <<< φ_{pNa+K}):

$$Na^+_{ex} + K^+_{ex} = (TBW * P_{Na+K} / f_{PW}) + (Na^+_{eA} + K^+_{eA}) + (Na^+_{eI} + K^+_{eI})$$

$$\varphi_{eNa+K} * \frac{Na^+_{ex} + K^+_{ex}}{TBW} = \varphi_{pNa+K} * P_{Na+K} / f_{PW} + \varphi_{pNa+K} * \frac{Na^+_{eA} + K^+_{eA}}{TBW}$$

$$\varphi_{eNa+K} * \frac{Na^+_{ex} + K^+_{ex}}{TBW} = \varphi_{pNa+K} \frac{Na^+_{ex} + K^+_{ex}}{TBW} - \varphi_{pNa+K} \frac{Na^+_{eI} + K^+_{eI}}{TBW}$$

A complete relationship for P_{Na} may be derived incorporating osmotically inactive Na^+ and K^+:[26]

$$P_{Na} = \frac{f_{PW} * m_{osm}}{\varphi_{pNa+K}} \left(\frac{\varphi_{eNa+K} * Na^+_{ex} + K^+_{ex}}{TBW} + \sum TB\,[s]_i * (\varphi_{tbi} - \varphi_{pi}/V_{Di}) \right) + \frac{f_{PW} * b_{[osm]}}{\varphi_{pNa+K}} - P_K$$

$$P_{Na} = f_{PW} * m_{osm} \frac{Na^+_{ex} + K^+_{ex}}{TBW} - f_{PW} * m_{osm} \left(\frac{Na^+_{eI} + K^+_{eI}}{TBW} - \frac{1}{\varphi_{pNa+K}} \sum TB\,[s]_i * (\varphi_{tbi} - \varphi_{pi}/V_{Di}) - \frac{b_{[osm]}}{m_{osm} * \varphi_{pNa+K}} \right) - P_K$$

We can also relate osmotically active excess cation to changes in $P_{Na+K,}$ non-Na^+ and K^+ osmoles, and $b_{[osm]}$:

$$\frac{Na^+_{eA} + K^+_{eA}}{TBW} = \frac{P_{Na+K} * (1 - m_{osm})}{f_{PW} * m_{osm}} - \frac{1}{\varphi_{pNa+K}} \left(\sum TB\,[s]_i * (\varphi_{tbi} - \varphi_{pi}/V_{Di}) + \frac{b_{[osm]}}{m_{osm}} \right)$$

The P_{Na} relationship appears complex, but if P_{Na} is plotted against $Na^+_{ex} + K^+_{ex}/TBW$, a linear relationship should result with a slope of f_{PW} * m_{osm} and a y-intercept determined by a balance between osmotically inactive excess Na^+ and K^+ against non-Na^+ and K^+ osmoles and a potential difference in plasma to total body osmolality. As expected changes in the osmotically inactive cation do not change P_{Na} since total exchangeable $Na^+ + K^+$ and inactive cation both change equally and cancel each other. Changes in osmotically active excess Na^+ and K^+ will either change the plasma to total body tonicity relationship (m_{osm} and/or $b_{[osm]}$) or non-Na^+ and K^+ solutes. P_{Na+K} changes minimally, since m_{osm} is close to 1 blunting P_{Na+K} impact on osmotically active excess cation.

In pioneering work, Edelman delineated a significant linear relationship between *molal* P_{Na} as the dependent variable and $(Na^+_e + K^+_e) \div TBW$ as the independent variable with a slope of 1.11 and a y-intercept of -25.6.[27] Other investigators note a weaker relationship between P_{Na} and $(Na^+_e + K^+_e) \div TBW$.[28-30] Conventional linear regression between P_{Na} and $(Na^+_e + K^+_e) \div TBW$ must be approached carefully as imprecise or inaccurate estimates may result due to non-normal distribution, narrow data range, and measurement error in the independent variable.[31] A reasonable analogy has been drawn to issues with linear regression to compare analytic methods in clinical laboratories, such as validation of a routine technique against a gold standard. Since both methods attempt to measure the same quantity, significant correlation is expected, but establishing whether such correlation translates into *quantitative* prediction of constant (y-intercept) and proportional (slope) differences between methods is often difficult. Since both independent and dependent variables are measured, measurement error in the independent variable is always present. Error in the independent variable tends to lower the slope and raise the y-intercept often termed dilution or attenuation bias.[32] Linear regression techniques adapted for independent variable measurement error may mitigate this issue. Indeed, Edelman's study recognized this issue and most likely used Deming linear regression to adjust for dilution bias.[31, 33] Some laboratory measurements such as plasma K^+ have inherently narrow data ranges which require large sample sizes to accurately determine method bias. Similarly, P_{Na} may range from 110 to 170 mEq/L or by a factor of

~1.5 requiring a sample size minimally greater than 100 and usually greater than 500-1000 to accurately determine equivalency.[34] While statistical variants of linear regression can reduce sample size requirements for narrow data sets, the resulting parameters often have broad confidence intervals. The ideal solution is a large enough sample size resulting in convergence of estimates from simple and complex linear regression algorithms.[35] Data transformation may expand the data range and reduce sample size requirements. In follow-up to the Edelman study, Boling and Olesen noted that the ($Na^+_e + K^+_e$) versus ($[Na^+ + K^+]_p$ * TBW) *total body cation* relationship improved linear regression probably due to a wider data set (~ 2500 – 10,000 mEq; factor of 4).[28, 30] Finally, P_{Na} data sets often exhibit positive skew as hyponatremia tends to be more commonly studied than hypernatremia; non-parametric linear regression such as Passing-Bablok may be useful in this circumstance.[36, 37]

Linear regression variations of the Edelman and pooled (Edelman, Boling, and Olesen) data sets are presented in Supplemental Table 2.[27, 28, 30] When the P_{Na+K} relationship is used, the simple linear regression estimates diverge significantly from the Deming and Passing-Bablok estimates suggesting inadequate sample size for the narrow data range. However, the slope and y-intercept estimates using the total body cation relationship are quite similar regardless of regression technique and reveals a slope of ~ 0.97 with *molal* $[Na^+ + K^+]_p$ and a y-intercept of about ~ 250 mEq. The P_{Na} relationship can now be simplified to:

$$P_{Na} = 1.03 * f_{PW} \quad \frac{Na^+_e + K^+_e - 250}{TBW} - P_K$$

The relationship delineates a m_{osm} of 1.03 and the net balance of osmotically inactive Na^+ and K^+ cation against non-Na^+ and K^+ solutes and plasma to total body osmolality difference ($b_{[osm]}$) to be about 250 mEq. m_{osm} is slightly greater than 1 suggesting that the ratio of exchangeable cation to TBW underestimates P_{Na}, while the negative y-intercept suggests the opposite. Only the interstitial and transcellular compartments are known to have cation concentrations below P_{Na+K}; thus these components must underlie the deviation of m_{osm} from the ideal of 1. All other compartments with cation concentrations higher than plasma must lead to the

overestimation of P_{Na} by the $(Na^+_{ex} + K^+_{ex}) \div TBW$ and contribute to the y-intercept. The non-Na^+ and K^+ plasma predominant osmoles (summation term negative) or a plasma and total body osmolality gradient (b[osm] negative with total body osmolality greater than plasma) primarily mirror osmotically active excess cation. In supplemental Table 3, we present compartments, estimate excess cation in these compartments, and delineate their effects on m_{osm} and the y-intercept of the P_{Na} relationship.

Translocational hyponatremia related to hyperglycemia (or other extracellular osmoles) is a common clinical situation where hyponatremia is not related to changes in exchangeable Na^+, K^+, or TBW, yet the P_{Na} relationship doesn't appear to account for these situations. Since the classic body composition studies examined euglycemic or mildly hyperglycemic patients, the narrow range of plasma glucose values prevented the investigators from delineating a relationship between P_{Na} and glucose.[27] To account for hyperglycemia, a revised relationship may be obtained:

$$P_{Na} = 1.03 * f_{PW} \left[\frac{Na^+_{ex} + K^+_{ex} - 250}{TBW} \right] - (G_{Na} * \Delta\,[Glucose]_p) - P_K$$

$$G_{Na} = \frac{1.03 * f_{PW} * [(\varphi_{tbGlucose} * V_{DGlucose}) - \varphi_{pGlucose}]}{\varphi_{pNa+K}}$$

where G_{Na} is a correction factor for hyperglycemia related translocational hyponatremia which has been proposed to range from 1.5 – 2.4 mEq/L per 100 mg/dL rise in plasma glucose ($\Delta\,[Glucose]_p$).[38-40]

Excess Na^+ and K^+ or non-Na^+ and K^+ solutes may change in pathologic states leading primarily to changes in the P_{Na} relationship y-intercept. The linear regression analysis yields a relatively fixed value for the y-intercept of 250 mEq (÷ TBW). The broad range of conditions in the study cohorts used for regression would suggest that excess Na^+ and K^+ is relatively fixed.[41] But edematous states seem overrepresented, while conditions such as SIADH, high sodium diet, volume depletion, and hyperglycemia are relatively absent.[27, 28, 30] Thus, the y-intercept in the P_{Na} relationship probably holds true for many disease states, but may not hold true for underrepresented states. For example, the y-intercept requires modification to account for hyperglycemia

due to shortcomings in the derivation cohorts.

At the bedside, clinicians use a shortcut for the P_{Na} relationship:[42, 43]

$$P_{Na} \cong \frac{Na^+_e + K^+_e}{TBW} - G_{Na} * \Delta\,[Glucose]_p$$

Error is a concern, but a slight variation minimizes error (< 5-10%) and is clinically useful to rationalize dysnatremias including pseudohyponatremia:

$$P_{Na} \cong f_{PW} * \frac{Na^+_e + K^+_e}{TBW} - (G_{Na} * \Delta\,[Glucose]_p) - P_K$$

Notably, this shorthand equation may be derived if one assumes plasma and total body tonicity equality (m_{osm} = 1 and b_{osm} = 0) with no osmotically inactive Na^+ and K^+ ($Na^+_{eI} + K^+_{eI} = 0$) and glucose representing the only non-Na^+ and K^+ effective osmole glucose ($\sum TB\,[s]_i * ((\varphi_{tbi} - \varphi_{pi}/V_{Di}) \div \varphi_{pNa+K}) = G_{Na} * \Delta\,[Glucose]_p$). As noted earlier, error may be significant if the y-intercept of the total body cation relationship changes with pathologic states (i.e. >> 250 mEq).

6. Estimation of Fixed Charge Density and Π_{GAG} for Skin Na^+ Storage

If 20-40 mEq/L of excess skin [Na^+] is completely stored in the interstitium, then the interstitial [Na^+] concentration must rise by a similar amount if we assume skin extracellular water is the vast majority of total skin water (>90%). Based on studies in cartilage,[44] an ideal Donnan equilibrium is likely to apply allowing a calculation of fixed charge density (FCD):

$$[Na^+]_{GAG} * [Cl^-]_{GAG} = [Na^+]_{if} * [Cl^-]_{if}$$

$$FCD = [Na^+]_{GAG} - [Cl^-]_{GAG}$$

where $_{GAG}$ and $_{if}$ represent ionic concentrations in the GAG and bathing interstitial fluid compartments respectively. If we let $[Na^+]_{if}$ and $[Cl^-]_{if}$ = 150 mEq/L (assuming equivalency of ions) and set $[Na^+]_{GAG}$ to 170-190 (i.e. 20-40 mEq/L > than 150 mEq/L), then FCD = 37.5 – 71.1 mEq/L. Π_{GAG} may be estimated assuming

ideal Donnan behavior:[45]

$$\Pi_{GAG} = \varphi_{NaCl} * RT * ([Na^+]_{GAG} + [Cl^-]_{GAG} - 2\,[Na^+]_{if} + [GAG])$$

$$\text{Assume } ([Na^+]_{GAG} + [Cl^-]_{GAG}) >>> [GAG] \text{ and } \varphi_{NaCl} \text{ at } 0.14\ M \cong 0.93$$

$$\Pi_{GAG} = 45 - 160 \text{ mm Hg } (2.5 - 8 \text{ mOsm/kg})$$

Alternatively, we can utilize an empirical equation derived from various proteoglycan preparations:[46, 47]

$$\Pi_{GAG} \text{ (mm Hg)} = 760\,[3.51 * (FCD/1000) + 19.3\,(FCD/1000)^2]$$

$$\Pi_{GAG} \text{ (mm Hg)} = 120 - 263 \text{ mm Hg } (6.2 - 13.6 \text{ mOsm/kg})$$

Supplemental Table 1. Plasma Protein MW_{av} Calculations in Low Albumin States. f_{alb} = albumin fraction of total protein (plasma albumin ÷ total protein). Normal patient limiting slopes adapted from references 14 and 11. Congenital analbuminemia data were derived using the data in reference 15: $f_{\alpha 1} = 0.13$ (normal ~ 0.033), $MW_{\alpha 1} = 45$ kD; $f_{\alpha 2} = 0.25$ (normal ~ 0.092), $MW_{\alpha 2} = 115$ kD; $f_{\beta} = 0.32$ (normal ~ 0.12), $MW_{\beta} = 125$ kD; and, $f_{\gamma} = 0.3$ (normal ~ 0.16), $MW_{\gamma} = 250$ kD (normal ~ 150 kD). The relative distribution of globulin fractions is significantly altered, but the molecular weights are normal except for MW_{γ}. Analbuminemic rat globulin slope estimated from reference 13. Nephrotic patient data calculated from reference [12] assuming $f_{alb} = 0.4$ (mean value of nephrotic cohort) and total protein limiting slope = 1.65 (determined by the authors). The resulting total protein slope and MW_{av} for $f_{alb} = 0.2$ in nephrotic syndrome also agrees with data from reference 16. Hypoalbuminemia data derived by assuming globulin limiting slope is slightly lower than congenital analbuminemia as serum protein profile is similar in these states.[13]

Condition	**Plasma Protein Fraction**	**$d\Pi / dc$ ($c = 0$)**	**MW_{av} (kD)**
Normal	Total Protein	2.1	92
	Albumin	2.8	69
	Globulin	1.3	149
Congenital Analbuminemia	Globulin (& total protein)	1.7	113
Nagase Analbuminemic Rat	Globulin (& total protein)	2	97
Nephrotic Patients	Albumin	2.8	69
	Globulin	0.9	215
	Total Protein ($f_{alb} = 0.4$)	1.65	117
	Total Protein ($f_{alb} = 0.3$)	1.47	132
	Total Protein ($f_{alb} = 0.2$)	1.28	151
Inflammatory Hypoalbuminemia	Albumin	2.8	69
	Globulin	1.6	121
	Total Protein ($f_{alb} = 0.4$)	2.1	92
	Total Protein ($f_{alb} = 0.3$)	2	97
	Total Protein ($f_{alb} = 0.2$)	1.84	105

Supplemental Table 2. Linear Regression Analaysis of Plasma and Body Tonicity Relationships. The Edelman and pooled data set of Edelman,[27] Boling,[28] and Olesen[30] were analyzed by ordinary linear regression, Deming regression (corrected for dilution bias), and Passing-Bablok regression (non-parametric) using Analyse-It for Microsoft Excel (version 2.20; Analyse-it Software, Ltd.; Leeds, U.K.). Values indicate means with 95% C.I. in parentheses. The $P_{Na} + P_K$ relationship clearly diverges amongst linear regression algorithms, while the Na^+_e and K^+_e relationship demonstrates similar estimates regardless of regression technique with improved confidence intervals particularly for the pooled data set. Using the $Na^+_e + K^+_e$ relationship for the pooled data set and averaging the three regression estimates yields a slope of 0.97 (2 out of the 3 estimates suggest the slope is statistically less than 1) and a y-intercept of 250 mEq.

Relationship: Molal $P_{Na} + P_K$ = Slope * [($Na^+_e + K^+_e$) ÷ TBW] + Y-intercept					
Edelman Data Set					
Ordinary		**Deming**		**Passing-Bablok**	
Slope	*Y-intercept*	*Slope*	*Y-Intercept*	*Slope*	*Y-Intercept*
0.92 (0.79 – 1.05)	7.11 (-12.21 – 26.43)	1.12 (0.96 – 1.28)	-21.8 (-45.0 – 1.43)	1.12 (0.99 – 1.30)	-21.8 (-48.0 - -2.3)
Pooled Data Set					
Ordinary		**Deming**		**Passing-Bablok**	
Slope	*Y-intercept*	*Slope*	*Y-Intercept*	*Slope*	*Y-Intercept*
0.69 (0.59 – 0.8)	44.0 (28.7 – 59.4)	0.98 (0.83 – 1.13)	1.53 (-21.2 – 24.2)	0.99 (0.87 – 1.12)	-1.17 (-20.5 – 17.7)
Relationship: $Na^+_e + K^+_e$ = Slope * [(Molal $P_{Na} + P_K$) * TBW] + Y-intercept					
Edelman Data Set					
Ordinary		**Deming**		**Passing-Bablok**	
Slope	*Y-intercept*	*Slope*	*Y-Intercept*	*Slope*	*Y-Intercept*
0.985 (0.955 – 1.015)	230 (67.3 – 392)	0.99 (0.95 – 1.04)	181 (-29 – 391)	1.02 (0.99 – 1.06)	35.5 (-132 – 186)
Pooled Data Set					
Ordinary		**Deming**		**Passing-Bablok**	
Slope	*Y-intercept*	*Slope*	*Y-Intercept*	*Slope*	*Y-Intercept*
0.96 (0.93 – 0.98)	299 (167 – 431)	0.97 (0.95 – 0.99)	232 (113 – 350)	0.98 (0.95 – 1)	222 (81 – 346)

Supplemental Table 3. Exchangeable Excess Cation Balance. Exchangeable excess cation concentration was calculated as estimated tissue exchangeable cation concentration (see Table 2) minus 154 mEq/L (estimated plasma cation concentration). Excess cation in mEq/kg was then calculated by multiplying excess concentration by compartment volume. Since the interstitial and transcellular compartments are the only known compartments with cation concentrations less than plasma, these were assumed to raise the slope (Δm), while all other compartments were assumed to modify the y-intercept of the P_{Na} relationship. The estimates are not exactly equal to the regression estimates from Supplemental Table 2, but are within the estimate error.

Compartment	**Excess Cation Concentration (mEq/L H_2O)**	**Volume (L/kg body weight)**	**Excess Cation (mEq/kg body weight)**	**Mechanism for Cation Excess**	**Δ m_{osm}**	**Δ Y-Intercept (mEq)**
Interstitial/ Transcellular	- 4	0.13	- 0.5	Hydrostatic Pressure	+ 0.006	-
Cartilage	100	0.012	1.44	Hydrostatic Pressure	-	- 88
Bone	250	0.012	3.6	Osmotic Inactivity	-	- 210
Intracellular	2	0.33	0.66	Osmotic Inactivity	-	- 48
Total		0.6	3.7		1.006	- 346

References

1. Watson, PE, Watson, ID, Batt, RD: Total body water volumes for adult males and females estimated from simple anthropometric measurements. *Am J Clin Nutr,* 33**:** 27-39, 1980.

2. Chumlea, WC, Guo, SS, Zeller, CM, Reo, NV, Baumgartner, RN, Garry, PJ, Wang, J, Pierson, RN, Jr., Heymsfield, SB, Siervogel, RM: Total body water reference values and prediction equations for adults. *Kidney Int,* 59**:** 2250-2258, 2001.

3. Ellis, KJ: Reference man and woman more fully characterized. Variations on the basis of body size, age, sex, and race. *Biol Trace Elem Res,* 26-27**:** 385-400, 1990.

4. Cass, A, Finkelstein, A: Water permeability of thin lipid membranes. *J Gen Physiol,* 50**:** 1765-1784, 1967.

5. Meyer, MM, Verkman, AS: Human platelet osmotic water and nonelectrolyte transport. *Am J Physiol,* 251**:** C549-557, 1986.

6. Alberts, B: *Molecular biology of the cell,* New York, Garland Science, 2008.

7. Odeh, YK, Wang, Z, Ruo, TI, Wang, T, Frederiksen, MC, Pospisil, PA, Atkinson, AJ, Jr.: Simultaneous analysis of inulin and 15N2-urea kinetics in humans. *Clin Pharmacol Ther,* 53**:** 419-425, 1993.

8. Walser, M, Bodenlos, LJ: Urea metabolism in man. *J Clin Invest,* 38**:** 1617-1626, 1959.

9. Basic anatomical and physiological data for use in radiological protection: reference values. A report of age- and gender-related differences in the anatomical and physiological characteristics of reference individuals. ICRP Publication 89. *Ann ICRP,* 32**:** 5-265, 2002.

10. Crone, C: The permeability of brain capillaries to non-electrolytes. *Acta Physiol Scand,* 64**:** 407-417, 1965.

11. Nitta, S, Ohnuki, T, Ohkuda, K, Nakada, T, Staub, NC: The corrected protein equation to estimate plasma colloid osmotic pressure and its development on a nomogram. *Tohoku J Exp Med,* 135**:** 43-49, 1981.

12. Canaan-Kuhl, S, Venkatraman, ES, Ernst, SI, Olshen, RA, Myers, BD: Relationships among protein and albumin concentrations and oncotic pressure in nephrotic plasma. *Am J Physiol,* 264**:** F1052-1059, 1993.

13. Kaysen, GA: Plasma composition in the nephrotic syndrome. *Am J Nephrol,* 13**:** 347-359, 1993.

14. Landis, EM, Pappenheimer, JR: Exchange of substances through the capillary walls. In: *Handbook of Physiology: Section 2: Circulation, Volume 2.* edited by HAMILTON, W. F., DOW, P., Washington, D.C., American Physiological Society; distributed by Williams & Wilkins, 1963.

15. Ott, H: [Blood serum in analbuminemia; further research on serum fractions, on the capacity to bind dyes and on the colloid-osmotic pressure]. *Z Gesamte Exp Med,* 128**:** 340-360, 1957.

16. Armstrong, SH, Jr., Kark, RM, Schoenberger, JA, Shatkin, J, Sights, R: Colloid osmotic pressures of serum proteins in nephrosis and cirrhosis: relations to electrophoretic distributions and average molecular weights. *J Clin Invest,* 33**:** 297-310, 1954.

17. Vavricka, SR, Burri, E, Beglinger, C, Degen, L, Manz, M: Serum protein electrophoresis: an underused but very useful test. *Digestion,* 79**:** 203-210, 2009.

18. Alper, CA: Plasma protein measurements as a diagnostic aid. *N Engl J Med,* 291**:** 287-290, 1974.

19. Elliott, JA, Prickett, RC, Elmoazzen, HY, Porter, KR, McGann, LE: A multisolute osmotic virial equation for solutions of interest in biology. *J Phys Chem B,* 111**:** 1775-1785, 2007.

20. Katchalsky, A: Polyelectrolytes and Their Biological Interactions. *Biophys J,* 4**:** SUPPL 9-41, 1964.

21. Kleinhans, FW, Mazur, P: Comparison of actual vs. synthesized ternary phase diagrams for solutes of cryobiological interest. *Cryobiology,* 54**:** 212-222, 2007.

22. Lietzke, MH, Stoughton, RW: Simple Method for Predicting Osmotic Coefficient of Aqueous-Solutions Containing More Than One Electrolyte. *J Inorg Nucl Chem,* 36**:** 1315-1317, 1974.

23. Prickett, RC, Elliott, JA, McGann, LE: Application of the osmotic virial equation in cryobiology. *Cryobiology,* 60**:** 30-42, 2010.

24. Khajuria, A, Krahn, J: Osmolality revisited--deriving and validating the best formula for calculated osmolality. *Clin Biochem,* 38**:** 514-519, 2005.

25. Knepper, MA, Sands, JM, Chou, CL: Independence of urea and water transport in rat inner medullary collecting duct. *Am J Physiol,* 256**:** F610-621, 1989.

26. Nguyen, MK, Kurtz, I: Quantitative interrelationship between Gibbs-Donnan equilibrium, osmolality of body fluid compartments, and plasma water sodium concentration. *J Appl Physiol,* 100**:** 1293-1300, 2006.

27. Edelman, IS, Leibman, J, O'Meara, MP, Birkenfeld, LW: Interrelations between serum sodium concentration, serum osmolarity and total exchangeable sodium, total exchangeable potassium and total body water. *J Clin Invest,* 37**:** 1236-1256, 1958.

28. Boling, EA, Lipkind, JB: Body Composition and Serum Electrolyte Concentrations. *J Appl Physiol,* 18**:** 943-949, 1963.

29. Moore, FD, Olesen, K.H., McMurrey, J.D., Parker, H.V., Ball, M.R., Boyden, C.M.: *The Body Cell Mass and Its Supporting Environment,* Philadelphia, W.B. Saunders, 1963.

30. Olesen, KH: Interrelations between total exchangeable sodium, potassium, body water, and serum sodium and potassium concentrations in hyponatremic and normonatremic heart disease. *Circulation,* 35**:** 895-903, 1967.

31. Nguyen, MK, Landaw, EM, Kurtz, I: Quantitative analysis of the dysnatremias. *Kidney Int,* 70**:** 1379-1381; author reply 1381-1372, 2006.

32. Hutcheon, JA, Chiolero, A, Hanley, JA: Random measurement error and regression dilution bias. *BMJ,* 340**:** c2289, 2010.

33. Deming, WE: *Statistical adjustment of data,* New York, John Wiley & Sons, 1943.

34. Linnet, K: Necessary sample size for method comparison studies based on regression analysis. *Clin Chem,* 45**:** 882-894, 1999.

35. Stockl, D, Dewitte, K, Thienpont, LM: Validity of linear regression in method comparison studies: is it limited by the statistical model or the quality of the analytical input data? *Clin Chem,* 44**:** 2340-2346, 1998.

36. Passing, H, Bablok: A new biometrical procedure for testing the equality of measurements from two different analytical methods. Application of linear regression procedures for method comparison studies in clinical chemistry, Part I. *J Clin Chem Clin Biochem,* 21**:** 709-720, 1983.

37. Twomey, PJ, Kroll, MH: How to use linear regression and correlation in quantitative method comparison studies. *Int J Clin Pract,* 62**:** 529-538, 2008.

38. Hillier, TA, Abbott, RD, Barrett, EJ: Hyponatremia: evaluating the correction factor for hyperglycemia. *Am J Med,* 106**:** 399-403, 1999.

39. Moran, SM, Jamison, RL: The variable hyponatremic response to hyperglycemia. *West J Med,* 142**:** 49-53, 1985.

40. Tzamaloukas, AH, Ing, TS, Siamopoulos, KC, Rohrscheib, M, Elisaf, MS, Raj, DS, Murata, GH: Body fluid abnormalities in severe hyperglycemia in patients on chronic dialysis: theoretical analysis. *J Diabetes Complications,* 21**:** 374-380, 2007.

41. Nguyen, MK, Kurtz, I: Is the osmotically inactive sodium storage pool fixed or variable? *J Appl Physiol,* 102**:** 445-447, 2007.

42. Rose, BD: New approach to disturbances in the plasma sodium concentration. *Am J Med,* 81**:** 1033-1040, 1986.

43. Mange, K, Matsuura, D, Cizman, B, Soto, H, Ziyadeh, FN, Goldfarb, S, Neilson, EG: Language guiding therapy: the case of dehydration versus volume depletion. *Ann Intern Med,* 127**:** 848-853, 1997.

44. Maroudas, A, Evans, H: A Study of Ionic Equilibria in Cartilage. *Connective Tissue Research,* 1**:** 69-77, 1972.

45. Overbeek, JT: The Donnan equilibrium. *Prog Biophys Biophys Chem,* 6**:** 57-84, 1956.

46. Urban, JP, Maroudas, A, Bayliss, MT, Dillon, J: Swelling pressures of proteoglycans at the concentrations found in cartilaginous tissues. *Biorheology,* 16**:** 447-464, 1979.

47. Basser, PJ, Schneiderman, R, Bank, RA, Wachtel, E, Maroudas, A: Mechanical properties of the collagen network in human articular cartilage as measured by osmotic stress technique. *Arch Biochem Biophys,* 351**:** 207-219, 1998.